THE EFFECT OF SPECIES DIFFUSION AND HEAT CONDUCTION ON NONEQUILIBRIUM FLOWS BEHIND STRONG SHOCKS

W.E. Gibson and J.D. Buckmaster
Contract No. NASr-119
CAL Report No. AG-1729-A-3
October 1963

CORNELL AERONAUTICAL LABORATORY, INC.
OF CORNELL UNIVERSITY, BUFFALO 21, N. Y.

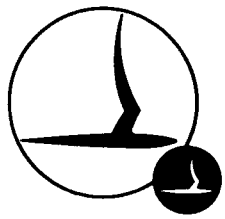

CORNELL AERONAUTICAL LABORATORY, INC.,
BUFFALO 21, NEW YORK

(NASA CR-55178; CAL REPORT NO. AG-1729-A-3) OTS: $5.60 pk, $1.94 mf

THE EFFECT OF SPECIES DIFFUSION AND HEAT CONDUCTION ON NONEQUILIBRIUM FLOWS BEHIND STRONG SHOCKS

(NASA CONTRACT NO. NASr-119)

OCTOBER 1963 58p

PREPARED BY: W. E. Gibson and J. D. Buckmaster

APPROVED BY: A. Hertzberg, Head
Aerodynamic Research Dep't

FOREWORD

The research reported in this report has been sponsored by the National Aeronautics and Space Administration under Contract NASr-119. The authors are pleased to acknowledge the capable help of Miss C. Rippey in the preparation of the paper. The computer program applied in Section III was written by Mr. S. R. Graczyk.

ABSTRACT

The effects of species diffusion and heat conduction are investigated for nonequilibrium flows behind strong, one-dimensional shocks. The relaxation zone is analyzed separately from the shock transition zone for translational (and rotational) temperature. It is shown that transport processes effectively decrease the high concentration and temperature gradients in the relaxation zone of strong shocks. This specific nonequilibrium behavior is studied for both vibration and dissociation. Strong effects are noted at shock speeds of 20 Kft/sec (for vibration) and 29 Kft/sec (for dissociation). Preliminary results are also given for airflows with coupled chemistry. Furthermore, a method for including the effects of free stream dissociation is presented for flows involving transport processes. The applications to bow shock flows at high re-entry speeds are pointed out.

TABLE OF CONTENTS

LIST OF SYMBOLS

Roman

A	scaling factor defined in Eqs. (48) and (50) for weak and strong diffusion respectively.
A_o	function defined in Eq. (31)
b	coefficient in viscosity formula, Eq. (19)
C	rate coefficient for a Lighthill gas, cf. Eq. (23)
d	constant in enthalpy equation, Eq. (39)
D	diffusion coefficient, cf. Eq. (3)
$F(\alpha, h)$	function defined in Eq. (26)
h	enthalpy parameter defined in Eq. (21)
$\mathcal{J}(\alpha; \Lambda, h)$	profile function defined in Eq. (37)
ℓ	reference length defined in Eq. (33)
ℓ'	relaxation length; see Eqs. (13)
n	collision number for relaxation, see Eq. (5)
$P(\alpha)$	rate function in Eq. (39)
p	gas pressure
q	flow velocity
$\mathcal{R}$	universal gas constant
s	temperature exponent of dissociation rate
Sc	Schmidt number, see Eq. (20)
T	gas temperature
T'	dimensionless temperature, see Eq. (20)
T_d	characteristic temperature of dissociation for a Lighthill gas
T_v	vibrational temperature
V_∞	speed of a normal shock

W_o	molecular weight of undissociated gas
y_n	population of quantum level (Appendix A)
γ	correlated concentration gradient defined in Eq. (25)

Greek

α	dissociation fraction
β	relaxation variable defined in Eq. (6)
γ_{SH}	adiabatic exponent immediately behind the transport shock
δ	collision diameter for elastic collisions, see Eq. (19)
$\Delta(\alpha)$	function defined in Eq. (32)
ϵ	concentration of excited species, see Eq. (4)
$\tilde{\epsilon}$	local equilibrium concentration of excited species, see Eq. (4)
η_{12}	scaling factor for subtraction rule, see Eq. (42)
Θ_v	characteristic temperature for vibration
Λ	parameter defined in Eq. (24)
μ	gas viscosity specified in Eq. (19)
ξ	dimensionless coordinate defined in Eq. (A-11)
ρ	gas density
σ	arc length along a streamline
σ'	dimensionless coordinate defined in Eq. (6)
Σ	dimensionless coordinate defined in Eq. (37)
τ	relaxation time, see Eq. (4)
$\Phi(T)$	rate function in Eq. (39)
$\Psi(x)$	energy function for vibration, see Eq. (A-3)
$\Omega^{2,2}$	collision integral, see Eq. (19)
$(\ )_{SH}$	indicates conditions immediately behind the transport shock
$(\ )_\infty$	indicates free stream properties
$\overline{(\ )}$	indicates the flight solutions ($\alpha_\infty = 0$) in Sections 3.4 and 4

I. INTRODUCTION

Shock wave structure has attracted much interest as the basic example of a high energy, nonequilibrium flow. Both elastic and inelastic collision processes are involved in the coupling of translational energy with rotation, vibration and chemical reactions. The nature of the coupling depends on shock strength.

For weak shocks, elastic collisions are much more frequent than inelastic ones so that the gas reaches translational equilibrium across a comparatively narrow zone. In the present report, this region of translational equilibration is called the "translation zone". At low temperatures, the narrow translation zone can be studied[2] independently of relaxation processes. The internal degrees of freedom remain frozen at their free stream values and the controlling physical effect is the elastic exchange of kinetic energy and momentum. This situation has been described[2] by various approximate solutions of the Boltzmann equation. Furthermore, the zone where relaxation occurs involves a continuum, inviscid flow. The initial conditions for the various relaxation processes are specified by the state of the gas after the translational transition. Our current studies of this zone include the coupling between vibration and dissociation.[3]

At high temperatures, the extrapolation[2, 4] of experimental data indicates a rapid decrease of the relaxation times for vibration and dissociation in airflows. Then, the division of shock structure into translation and relaxation zones must be carefully checked. Two questions should be asked about the relaxation zone. Does it depend on the structure of the translation zone? Is the flow inviscid?

The first question is considered in Refs. 2 and 5-7. The estimates of Ref. 2 and the solutions of Refs. 5 and 6 suggest that relaxation of vibration and

dissociation never develops before the end of the translation zone. Even rotational relaxation is independent of the structure of the translation zone, as demonstrated by the solution of Ref. 7. Further estimates given in the present report (Section 2.3) support these conclusions.

To answer the second question, one need only examine available inviscid solutions. For example, at a lunar reentry speed,[8] the relaxation zone shows such extreme concentration gradients that species diffusion must become important. Concurrently, the translational temperature drops very quickly because the thermal energy is very rapidly transformed into chemical energy. As a result, heat conduction cannot be neglected. In this noteworthy situation, species diffusion and heat conduction are enhanced by the nonequilibrium nature of the flow.

This situation is studied here. The effects were not included in previous studies concerned with electron diffusion ahead of the shock.[9,10] Furthermore, species diffusion was neglected (zero Lewis number) in the early work of Ref. 5 which treats oxygen dissociation in air at a shock speed of 20 Kft/sec. In the present report, species diffusion and heat conduction are found to have important effects on the relaxation zone at shock speeds of 20 Kft/sec or more, depending on the chemical species.

The model for a strong shock assumes that the translational transition is completed before any significant relaxation occurs. This is consistent with the previous results discussed above. However, species diffusion and heat conduction are now allowed in the relaxation zone. Analytic and numerical solutions are obtained for simplified chemical models. The upstream boundary of the relaxation zone is defined by matching the concentration profile with a

pure diffusion solution. This latter solution applies within the translation zone, where relaxation rates are neglected by virtue of the basic assumption.

The analysis of the relaxation zone is further simplified by dropping terms of order $\frac{\rho_\infty}{\rho_{SH}} \ll 1$, ρ_∞ and ρ_{SH} being, respectively, the free-stream density and the density immediately behind the translation zone. Thus, momentum flux and momentum transport are neglected as higher order effects so that the pressure remains constant. Accordingly, pressure diffusion is not included. Thermal diffusion is also ignored, as suggested by the results of Ref. 11. The Lewis number is assumed to be unity so that species diffusion and heat conduction are given equal importance. Hence the gas enthalpy is not affected[12] by species diffusion and heat conduction, i. e. the enthalpy remains equal to its post translation zone value, to order $\left(\frac{\rho_\infty}{\rho_{SH}}\right)^2$. Finally, it should be noted that continuum flow is assumed in the relaxation zone.

It is interesting to compare the present study with the work of Refs. 13 and 14. These references account for transport processes in blunt body flows with cold walls near the free molecule limit. Then, nonequilibrium relaxation processes are not an essential feature of the problem. In fact, wall cooling depresses the reaction rates and effectively cancels the specific nonequilibrium behavior analyzed here. Species diffusion is important in Ref. 14 because of large mean free paths rather than because of high concentration gradients. In both Ref. 14 and the present report, it is shown that upstream diffusion creates finite concentrations of excited species immediately behind the translation zone.

The body of this report comprises three Sections. Section II gives the solution for a linearized model which displays the effect of species diffusion in a simple manner. Section III is devoted to a nonlinear theory for the Lighthill

gas[15] including both species diffusion and heat conduction. Analytic and numerical solutions are obtained. The subtraction rule of Ref. 1 for free stream dissociation is extended to flows involving diffusion and conduction. Finally, Section IV presents the conclusions. Applications to air flows with coupled chemistry and to blunt-body flows are discussed in Appendix B and Section IV.

II. LINEARIZED THEORY

Introduction

This Section involves a single, linearized rate equation with species diffusion. The rate equation is analyzed behind the translation zone of a normal shock where the gas is assumed to be in translational equilibrium.* The results demonstrate the importance of species diffusion when the reaction rate is large. They are applied to vibrational relaxation in oxygen and nitrogen. Furthermore, the basic division of the shock structure into translation and relaxation zones is validated by means of numerical examples.

2.1 Flow Model

The one dimensional flow behind the translation zone has a constant mass flux and a nearly uniform pressure

$$\rho q = \rho_\infty V_\infty , \qquad p \approx p_{SH} = \frac{2}{\gamma_{SH}+1}\ \rho_\infty V_\infty^2 \tag{1}$$

In Eqs. (1), the subscript " ∞ " denotes free stream properties and "SH" indicates properties immediately behind the translation zone. Density changes are neglected in the linearized treatment of the relaxation zone, so that

$$\frac{\rho}{\rho_\infty} \simeq \frac{\rho_{SH}}{\rho_\infty} = \frac{\gamma_{SH}+1}{\gamma_{SH}-1} \tag{2}$$

In addition, the Schmidt number (or Prandtl number for diffusion) is set equal to one, although any constant value could be retained. Hence, the diffusion coefficient is

---

*Rotational equilibrium is also assumed behind the translation zone, since rotational relaxation is not of particular interest here.

$$D = \frac{\mu}{\rho} \tag{3}$$

These assumptions simplify the analysis without compromising its general significance.

Upon inclusion of the diffusion term and application of Eq. (3), the relaxation equation is given by[16]

$$q \frac{d\epsilon}{d\sigma} - \frac{1}{\rho} \frac{d}{d\sigma} \left(\mu \frac{d\epsilon}{d\sigma} \right) = \frac{\tilde{\epsilon} - \epsilon}{\tau} \tag{4}$$

where ϵ, $\tilde{\epsilon}$ and σ are, respectively, the local concentration of excited species, the local equilibrium concentration, and the distance from the downstream boundary of the translation zone ($\sigma_{SH} = 0$). For vibrational relaxation, ϵ can represent the average vibrational energy of the gas and Eq. (4) then accounts for the diffusion of vibrationally excited molecules. (See Appendix A and Section 2.3). For a dissociation process, ϵ represents the atom concentration and Eq. (4) includes the rate of atom diffusion. In both cases, the relaxation time, τ, is conveniently expressed in terms of an average number of collisions for relaxation, say η. The relaxation time τ is then given by $\frac{\eta \lambda}{a}$, where λ and a are respectively the mean free path for elastic collisions, and the mean thermal speed. Applying $\lambda = \frac{2\mu}{\rho a}$ and $a = \sqrt{\frac{8p}{\pi\rho}}$, one finds[7]

$$\tau = \frac{\pi}{4} \frac{\mu}{p} \eta \tag{5}$$

In the present analysis, $\tilde{\epsilon}$ and η are assumed constant (so that $\tilde{\epsilon} = \tilde{\epsilon}_{SH}$). This differs somewhat from the usual treatment[17] of linearized theory where the variations of $\tilde{\epsilon}$ are allowed. For vibrational relaxation, the assumption of constant $\tilde{\epsilon}$ is justified in Appendix A. For dissociation,

the case of primary interest corresponds to high temperatures and low densities, i.e. to a situation where the local equilibrium is given by full dissociation, $\tilde{\epsilon} = 1$. Since the viscosity is a weak function of temperature and of ϵ, the assumption of constant η is only slightly less restrictive than that of constant relaxation time. Thus, the physical situation considered here is essentially that of relaxation in a heat bath. The heat bath solution is further examined in Section III.

Two new variables are now introduced in Eq. (4), namely

$$\beta = \frac{\epsilon}{\tilde{\epsilon}_{SH}} , \qquad \sigma' = \int_0^{\sigma} \frac{\rho}{D} \, d\sigma \tag{6}$$

In the present case, σ' is equal to $\frac{\pi(\gamma_{SH}-1)}{8}$ times the number of collisions experienced by a gas particle in the relaxation zone from 0 to σ. After application of Eqs. (1), (2), (5) and (6), Eq. (4) reduces to

$$\frac{d\beta}{d\sigma'} - \frac{d^2\beta}{d\sigma'^2} = \frac{8}{\pi(\gamma_{SH}-1)} \frac{1}{n}(1-\beta) \tag{7}$$

To determine a unique solution of Eq. (7), two boundary conditions are required. Let β_∞ be the free stream value for β, i.e. the value prescribed ahead of the translation zone. Far behind the translation zone, the rate process reaches equilibrium. Hence, one has

$$\begin{aligned} \sigma' = -\infty &: \beta = \beta_\infty = \frac{\epsilon_\infty}{\tilde{\epsilon}_{SH}} \\ \sigma' = +\infty &: \beta = 1 \end{aligned} \tag{8}$$

According to the present model, the relaxation rate is neglected upstream of the relaxation zone, i.e. the translation zone and ahead of it. In this region, Eq. (7) can be integrated to give

$$\beta - \beta_\infty = \frac{d\beta}{d\sigma'} \qquad \text{for} \quad \sigma' \leq 0 \tag{9}$$

The solution of Eq. (9) predicts an exponential decay to β_∞ as $\sigma' \longrightarrow -\infty$. At $\sigma' = 0$, the $\beta(\sigma')$ profile must be continuous. Thus, Eq. (9) and the second Eq. (8) provide the boundary conditions for the relaxation zone

$$\sigma' = 0 : \beta_{SH} = \beta_\infty + \left(\frac{d\beta}{d\sigma'}\right)_{SH} \tag{10}$$

$$\sigma' = +\infty : \beta = 1$$

The boundary condition at the shock includes a transport term, $\left(\frac{d\beta}{d\sigma'}\right)_{SH}$, which is analogous to that introduced in Ref. 14 for blunt body flows. Here, the transport effect arises specifically from the relaxation process rather than from the influence of a cold wall. As shown in Section 2.2, the inviscid limit, $\beta_{SH} = \beta_\infty$, is recovered when η is large, i.e., when the relaxation time is long. For small η, the transport term in Eqs. (10) becomes much larger than β_∞ and the relaxation process is strongly modified by diffusion.

2.2 Solution of the Linearized Rate Equation

The exact solution of Eqs. (7) and (10) is

$$\frac{1-\beta}{1-\beta_{SH}} = \exp\left(-\frac{\sigma'}{\ell'}\right) \tag{11}$$

where the relaxation length, ℓ', and the concentration at the shock are found to be

$$\ell' = 2\left[\left(1 + \frac{32}{\pi(\gamma_{SH}-1)}\,\frac{1}{\eta}\right)^{1/2} - 1\right]^{-1} \tag{12}$$

$$\frac{\beta_{SH} - \beta_\infty}{1-\beta_\infty} = \frac{1}{1+\ell'} \tag{13}$$

The effect of species diffusion is displayed by the dependence of ℓ' and β_{SH} on η . If η is large, the inviscid solution is recovered, corresponding to the neglect of $\frac{d^2\beta}{d\sigma'^2}$ in Eq. (7). Equations (12) and (13) then reduce to

$$\ell' \longrightarrow \frac{\pi}{8}\,\eta\,(\gamma_{SH}-1), \qquad \beta_{SH} \longrightarrow \beta_\infty \qquad \text{for } \eta \gg 1 \tag{14}$$

and exactly η collisions are required to decrease $\frac{1-\beta}{1-\beta_{SH}}$ from 1 to $\frac{1}{e}$. On the other hand, if η is small, the diffusion term becomes dominant in the left hand side of Eq. (7) giving for small η

$$\ell' \longrightarrow 2\sqrt{\frac{\pi}{8}\,\eta\,(\gamma_{SH}-1)}\ , \qquad \beta_{SH} \longrightarrow \beta_\infty + \frac{1-\beta}{1+2\sqrt{\frac{\pi}{8}\,\eta\,(\gamma_{SH}-1)}} \tag{15}$$

Then, diffusion is an important mechanism for equilibration and the required number of collisions is $\sqrt{\frac{8\eta}{\pi(\gamma_{SH}-1)}}$. Generally, as η decreases, both $\frac{1}{\ell'}$ and β_{SH} increase so that β increases for any fixed value of σ' . It can also be verified that diffusion decreases the concentration gradients.

As a realistic example, consider the range $10 \leq \eta \leq 100$ with $\gamma_{SH} = 7/5$. For η = 100, one finds ℓ' = 16.67 in excellent agreement with the first Eq. (14). For η = 10, the exact solution gives ℓ' = 2.27 whereas the first Eq. (14) is still more accurate (ℓ' = 1.58) than the strong diffusion value, ℓ' = 1.31. Thus, the inviscid solution for the relaxation length is essentially valid for $\eta \geq 10$. On the other hand, the concentration at the shock is appreciably modified by diffusion since the factor $\frac{1}{1+\ell'}$ increases from 0.06 (for η = 100) to 0.30 (for η = 10). The conclusion is that, for $\eta \geq 10$, species diffusion modifies the inviscid profile effectively as an increase in free stream concentration. It should be recalled that heat conduction has no effect in the present model, since the relaxation time remains essentially constant.

The effective increase in free stream concentration is defined by Eq. (13). It is most marked when β_∞ is small, as occurs for a vibrationally cold or undissociated free stream. Furthermore, if η is kept the same, the ratio $\frac{1-\beta_{SH}}{1-\beta_\infty}$ remains constant.

$$\frac{1-\beta_{SH}(\beta_\infty)}{1-\beta_\infty} = \frac{1-\beta_{SH}(\beta'_\infty)}{1-\beta'_\infty} \tag{16}$$

for any choice of β_∞ and β'_∞. If β_∞ and β'_∞ are small, Eq. (16) reduces to a subtraction rule similar to that of Ref. 1

$$\beta_{SH}(\beta_\infty) - \beta_\infty \approx \beta_{SH}(\beta'_\infty) - \beta'_\infty \approx \beta_{SH}(0) \tag{17}$$

Equations (16) and (17) are extended in Section III for a nonlinear relaxation equation.

2.3 Vibrational Relaxation

The effect of species diffusion on vibrational relaxation behind a translational (and rotational) zone is now evaluated by applying the general solution, Eqs. (11) and (12). The validity of the flow model will also be studied.

The model for vibrational relaxation is that proposed in Ref. 18 for diatomic molecules. The rate equation is derived in Appendix A where the only difference from the analysis of Ref. 18 is the inclusion of a transport term. This term describes the interdiffusion of vibrationally excited molecules. It is found to have an important effect at high temperatures.

As shown in Appendix A, the rate equation is given by Eq. (7) with σ' and β defined as in Eqs. (6) and ϵ equal to the average vibrational energy. In fact, if both vibrational and translation temperatures are high, β is equal to the ratio of vibrational to translational temperature (fully excited equilibrium vibration). Three gas mixtures are considered in the computations, namely pure O_2, pure

N_2, and O_2 in a bath of Argon. The corresponding relaxation times are given by extrapolations of experimental data[19, 20]

$$\tau_{O_2} p = 1.6 \times 10^{-9} \exp\left(\frac{101.44}{T^{1/3}}\right)$$

$$\tau_{N_2} p = 1.1 \times 10^{-11} T^{1/2} \exp\left(\frac{154}{T^{1/3}}\right) \qquad (18)$$

$$\tau_{O_2\text{-}Ar} = 1.1 \times 10^{-15} T^{5/6} \left[1 - \exp\left(-\frac{2228}{T}\right)\right]^{-1} \times \exp\left(\frac{1.04 \times 10^{7}}{T}\right)^{1/3}$$

In Eqs. (18), τ , p and T are measured in seconds, atmospheres, and °K, respectively. The respective viscosity coefficients are approximated by the kinetic formula for a monatomic gas

$$\mu = b\sqrt{T}, \qquad b = \frac{2.7 \times 10^{-5} \sqrt{W_0}}{\delta^2 \Omega^{2,2}(T)} \qquad (19)$$

The data for the collision diameter δ (in Å) and the collision integral $\Omega^{2,2}$ are obtained from Ref. 16. Finally, γ_{SH} is set equal to 7/5 for O_2 and N_2 and to 5/3 for the Argon bath.

As shown in Eq. (12), the governing parameter of the problem is the collision number, η . For vibrational relaxation of a given mixture, η depends only on the translational temperature (cf Eqs. (5), (18) and (19)). The function $\eta(T)$ is plotted in Fig. 1 for the three mixtures over a range of 5000°K $\leq T \leq$ 30,000°K. As T increases, η decreases rapidly because the increase of μ with temperature is overwhelmed by the strong decrease of τ . In fact, the curves of Fig. 1 are ordered according to the relaxation times, reflecting the decreasing collision efficiencies of O_2, Ar and N_2 at a given temperature. It should be noted that η never falls below 10 in the range considered. This fact will be used below to justify the flow model adopted here.

Consistent with linearized theory, the value of η in Eqs. (12) and (13) is evaluated at the translational temperature for frozen vibration. This is rigorously

correct for the Argon bath and is found to be quite accurate for pure O_2 and N_2. Figure 2 shows the vibrational temperature, $T_{v,SH}$, immediately behind the translation zone as a function of shock speed. The data correspond to a vibrational temperature $T_{v_\infty} = 300°K$ in the free stream. The computation is based on Eqs. (12), (13) and Eq. (A-3). For inviscid flow, one has

$$T_{v,SH} = T_{v_\infty} = 300°K$$

The large effect of diffusion is apparent at shock speeds higher than 10^4 ft/sec. As V_∞ increases, so does the ratio $\frac{T_{v,SH}}{T_{SH}}$, T_{SH} being the translational temperature at the shock. The significance of these results must, of course, be evaluated in view of the limited validity of the extrapolations used in Eqs. (18).

The order of the three curves in Fig. 2 should also be noted. At fixed shock speed, T_{SH} is essentially the same for O_2 and N_2 and the higher value for $T_{v,SH}(O_2)$ reflects only the lower value for $\eta(O_2)$. However, T_{SH} is appreciably higher for the Argon bath (higher values of γ_{SH} and W_o) and, consequently, the order of the three curves is different from that observed in Fig. 1.

Since large effects of diffusion are predicted for a realistic range of shock strengths, it appears worthwhile to study the flow model in more detail. Two points should be considered, namely the accuracy of the linearized theory and the validity of the division into translation and relaxation zones. The application of linearized theory in the relaxation zone is shown to be quite accurate in Appendix A. The other, more important point is examined here on the basis of the results of Ref. 7.

In the model of Ref. 7, a single relaxation mode is coupled with the translation zone. However, species diffusion is neglected. The collision number for relaxation, η, is assumed constant so that a direct comparison is possible with

the present work. Several values of η are considered for strong shocks. Even for the low value, $\eta = 10$, the data given in Ref. 7 suggest that the relaxation zone is effectively uncoupled from the translation zone (see Fig. 10 of Ref. 7). The situation is indicated in the sketch below.

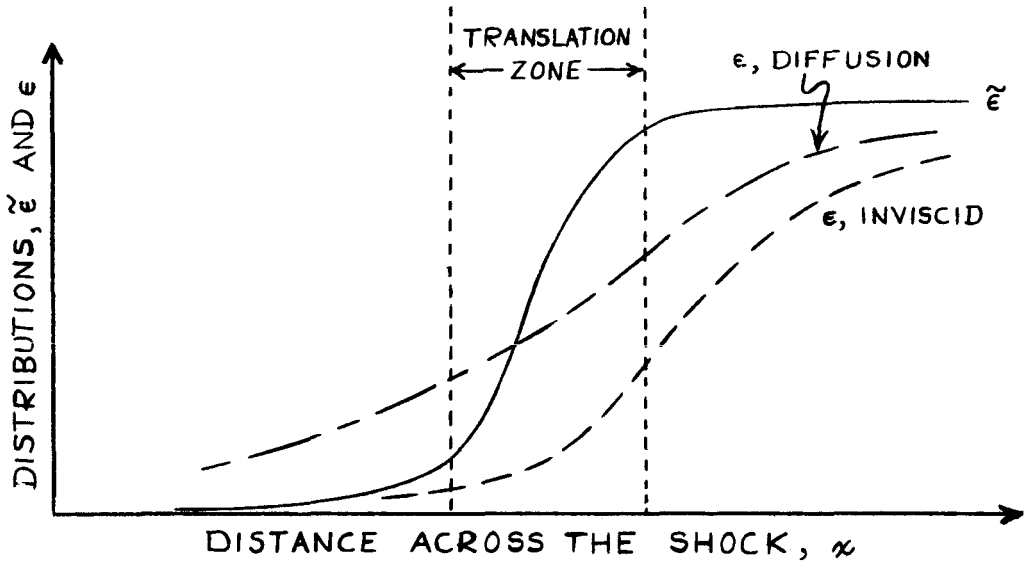

The full curve represents the local equilibrium, $\tilde{\epsilon}(T)$ in the notation of Section 2.1. The profile $\tilde{\epsilon}(x)$ is essentially independent of the relaxation process because the enthalpy and density changes involved in the relaxation process are small. The lower, dashed curve represents a typical nonequilibrium profile, $\epsilon(x)$, computed in Ref. 7. It is apparent that the main rise of $\tilde{\epsilon}$ occurs earlier than that of ϵ, i.e., that shock heating precedes internal excitation. Thus, the rate term $\frac{\tilde{\epsilon} - \epsilon}{\eta}$ has a negligible effect within the translation zone in agreement with the model applied in the present report. This is not surprising because the translation zone involves appreciably less than 10 collisions.

The conclusion is not modified by species diffusion. The upper dashed curve in the sketch typifies the present solution including diffusion behind the translational

zone. It is seen that diffusion actually decreases $\frac{\tilde{\epsilon} - \epsilon}{\eta}$, since ϵ is increased for fixed α . If the energy balance were considered, the translational temperature T and, hence, $\tilde{\epsilon}$ would also be decreased by diffusion. Thus, the validity of the present model is enhanced by species diffusion. It should be noted that ϵ can exceed $\tilde{\epsilon}$ in the early part of the shock. The above conclusions are a fortiori valid for dissociation since the latter does not proceed until an incubation time for vibration[3, 20] has elapsed.

In conclusion, the present analysis indicates a large effect of diffusion on vibrational relaxation in a strong normal shock. In particular, the vibrational temperature immediately behind the translation zone can be increased to a high value due to upstream diffusion of excited molecules.

III. ANALYTIC AND NUMERICAL SOLUTIONS FOR A LIGHTHILL GAS

Introduction

The rate equation solved in the present Section includes the variation of relaxation time with local temperature and concentration which was neglected in the linearized theory of Section II. Thus, species diffusion and heat conduction are both involved in the solution. The problem treated is the dissociation of the Lighthill gas. Analytic solutions are given for a range of values of the rate coefficient which comprises the transition from an inviscid flow to one controlled by diffusion. Numerical solutions are also obtained. The case of air flows with coupled chemistry is briefly discussed in Appendix B. The effect of dissociation in the free stream is considered and the subtraction rule of Ref. 1 is extended to flows involving species diffusion.

3.1 Flow Model

Equations (1) remain valid behind the transport zone. However, in the present treatment, density variations in the relaxation zone are accounted for. Furthermore, the Schmidt number may now differ from unity, so that the diffusion coefficient is given by

$$D = \frac{\mu}{\rho} \, Sc \tag{20}$$

The Lewis number is assumed to be unity. Thus, the enthalpy of the gas remains essentially constant $\left(\frac{q}{V_\infty} \ll 1 \quad \text{in the relaxation zone}\right)$ even when diffusion is important. The enthalpy of a Lighthill gas[15] is given by

$$h = (4 + \alpha)\, T' + \alpha \,, \qquad T' = \frac{T}{T_d} \tag{21}$$

with the enthalpy parameter

$$h = \frac{W_0 V_\infty^2}{2 \mathcal{R} T_d} + \alpha_\infty \tag{22}$$

The free stream concentration, α_∞ in Eq. (22), is set equal to zero in the solutions unless otherwise specified.

The viscosity coefficient is approximated by the value given in Eq. (19) for the undissociated gas. Indeed, the rather weak dependence of μ on α is not a basic feature of reacting flows.[21] Furthermore, three-body recombination can be neglected in the relaxation equation[22] because the final equilibrium level reaches full dissociation at the high shock speeds of present interest. The dissociation rate is taken to be

$$C\rho(1-\alpha)T^{-s}\exp\left(-\frac{T_d}{T}\right)$$

in conformity with the classical notation for a Lighthill gas. Equations (1), (6), (20) and (21) and the equation of state are combined with the relaxation equation, giving

$$\frac{d\alpha}{d\sigma'}-\frac{d^2\alpha}{d\sigma'^2}=\frac{CW_o^2V_\infty^2Sc}{\mathcal{R}^2T_d^{s+2}}\mu\left(\frac{2}{\gamma_\infty+1}\right)^2\frac{1-\alpha}{(1+\alpha)^2}T'^{-(s+2)}\exp\left(-\frac{1}{T'}\right) \tag{23}$$

$$T'=\frac{h-\alpha}{4+\alpha}$$

Since the local equilibrium concentration ($\tilde{\epsilon}$ in Section II) is equal to unity, β now becomes equal to the dissociation fraction α .

Next, Eq. (19) is substituted into Eqs. (23) and a controlling parameter of the problem is defined

$$\Lambda=\frac{bCW_o^2V_\infty^2Sc}{\mathcal{R}^2T_d^{5+3/2}} \tag{24}$$

where, for simplicity, the viscosity coefficient b and the Schmidt number Sc are assumed constant. As shown below, it is useful to scale the profile slope by $\sqrt{\Lambda}$. Consequently, a new unknown function is introduced

$$y=\frac{1}{\sqrt{\Lambda}}\frac{d\alpha}{d\sigma'} \tag{25}$$

Equations (23) reduce to a first order differential equation for $\mathcal{Y}(\alpha; \Lambda, h)$ because the variable σ' is not explicitly involved. This simplification is due to the fact that the normal shock flow defines its own length scale. One obtains the basic formulation

$$\left(\frac{1}{\sqrt{\Lambda}} - \frac{d\mathcal{Y}}{d\alpha}\right)\mathcal{Y} = (1-\alpha)\,F(\alpha,h)$$
$$F(\alpha,h) \equiv \frac{1}{(1+\alpha)^2}\left(\frac{4+\alpha}{h-\alpha}\right)^{s+3/2} \exp\left(-\frac{4+\alpha}{h-\alpha}\right) \tag{26}$$

The boundary conditions for Eq. (26) are derived from Eqs. (10), namely

$$\sigma' = 0 : \frac{d\alpha}{d\sigma'} = \mathcal{Y}(\alpha_{SH}, \Lambda)\sqrt{\Lambda} = \alpha_{SH} - \alpha_\infty$$
$$\sigma' = \infty : \alpha = 1, \quad \mathcal{Y} = 0 \tag{27}$$

In fact Eq. (26), being of first order in $\mathcal{Y}$, requires only one boundary condition which is chosen to be the second Eq. (27). Once the singular solution of Eq. (26) $\alpha = 1$, $\mathcal{Y} = 0$ is discarded, the second Eq. (27) specifies a unique, physically acceptable solution for $\mathcal{Y}(\alpha, \Lambda)$. The first Eq. (27) only serves to determine α_{SH}.

3.2 Analytic Solutions

Consider, first, the limiting cases of inviscid flow and of flow with strong diffusion. Since the parameter Λ is proportional to the ratio of the cross-sections for inelastic (dissociation) and elastic collisions, small values of Λ correspond to a weak effect of diffusion. Indeed, for small Λ, Eqs. (26) yield the inviscid solution

$$\mathcal{Y} = (1-\alpha)\sqrt{\Lambda}\; F(\alpha, h) \tag{28}$$

On the other hand, for large Λ, Eqs. (26) reduce to

$$-\mathcal{Y}\frac{d\mathcal{Y}}{d\alpha} \approx (1-\alpha)\; F(\alpha, h) \tag{29}$$

Thus, the Λ-dependence of $\mathcal{Y}$ disappears for strong diffusion. This behavior motivated the choice made in Eq. (25).

To derive an analytic solution of Eqs. (26), it is helpful to start with a simple case where the rate function $F(\alpha, h)$ is approximated by a constant mean value

$$F(\alpha, h) \approx F_m \tag{30}$$

The corresponding physical situation is that of dissociation in a heat bath [$F(\alpha, h)$ is primarily dependent on temperature which remains constant for the heat bath]. Equations (26) then have an exact solution

$$\mathcal{Y} = (1-\alpha)\, A$$

$$A = A_0(F_m) = \frac{1}{2}\left\{\left(4F_m + \Lambda^{-1}\right)^{1/2} - \Lambda^{-1/2}\right\} \tag{31}$$

As expected, the function $A_0(F_m)$ is simply related to the relaxation length ℓ' of the linearized theory (cf. Eq. (12)). One has

$$\ell' = \frac{1}{\gamma\Lambda\, A_0(F_m)}$$

$$\eta = \frac{8}{\pi(\gamma-1)}\,\frac{1}{\Lambda F_m}$$

Equations (31) also apply when $F(\alpha, h)$ varies slowly with α, provided F_m is replaced by the local value $F(\alpha, h)$. A correction term of order $\frac{\partial F}{\partial \alpha}$ is easily included as follows. Equations (31) are substituted into Eqs. (26), giving an exact relation for A.

$$A - \frac{F}{A} + \Lambda^{-1/2} = (1-\alpha)\,\frac{\partial A}{\partial \alpha}$$

Next, using a perturbation expansion,

$$A = A_0(F) + \frac{(1-\alpha)\, A_0(F)\,\Lambda^{1/2}}{1 + 2A_0(F)\Lambda^{1/2}}\,\frac{\partial A_0}{\partial \alpha} + \cdots$$

or

$$\chi = (1-\alpha)\, A_0 \left[\alpha + \Delta(\alpha)\right]$$

$$\Delta(\alpha) = \frac{(1-\alpha)\, A_0 \left[F(\alpha, h)\right] \Lambda^{1/2}}{1 + 2 A_0 \left[F(\alpha, h)\right] \Lambda^{1/2}} \qquad (32)$$

This result provides a simple analytic solution. For weak diffusion $(\Lambda \to 0)$, Eqs. (32) agree with the exact solution up to order $\Lambda^{5/2}$. For strong diffusion $(\Lambda \gg 1)$, Eqs. (32) are subject to an error of order $\frac{\partial^2 F(\alpha, h)}{\partial \alpha^2}$ as may be checked by substitution into Eq. (29). In fact, Eqs. (32) are in good agreement with the exact numerical solution obtained below for $\Lambda \geq 1$. This is shown by the following table in which the analytic solution for $\chi(\alpha = 0, h)$ is compared with the exact solution (h = 3.0).

TABLE 1

Λ	1	10	10^2	10^3	∞
$A_0[\Delta(0)]$	0.23	0.33	0.39	0.41	0.42
Exact	0.26	0.39	0.46	0.48	0.50

The maximum error of the approximate solution does not exceed 16%. For other values of α and h, the agreement is equally good. This is not surprising in view of the physical validity of the analytic solution. Indeed, at high enthalpies, neither the temperature nor the chemical rate vary strongly with α so that the heat bath approximation is valid. At low enthalpies where diffusion is less important, the inviscid solution is identically recovered by Eqs. (32).

In summary, the relaxation equation for nonequilibrium diffusive flow behind a normal shock has a simple analytic solution which describes accurately the transition from weak to strong diffusion as the rate coefficient is increased.

3.3 Exact Solutions and Results

Exact Solutions for A Lighthill Gas

The exact solution of Eqs. (26)is obtained by numerical integration starting from the equilibrium limit, $\alpha = 1$, with $A = \frac{\gamma}{1-\alpha}$ as an auxiliary unknown. For $\Lambda \geq 10$, the numerical scheme is found to be stable. For $\Lambda < 10$, a numerical instability arises near $\alpha = 1$. It is circumvented by applying Eqs. (32) over a small interval $\alpha_1 \leq \alpha \leq 1$. The effect of varying α_1 between 0.95 and 0.99 is found to be negligible.

Once $\gamma(\alpha, h)$ is known, the concentration profile is obtained from

$$\frac{\sigma}{l} = \int_{\alpha_{SH}}^{\alpha} \frac{\sqrt{T'}}{\gamma}\, d\alpha$$
$$l = \frac{\rho_\infty V_\infty \sqrt{\Lambda}}{b\sqrt{T_d}} \qquad (33)$$

where α_{SH} is the concentration at the upstream boundary of the relaxation zone. Furthermore, α_{SH} is determined by the first Eq. (27).

Effect of Diffusion for A Lighthill Gas

The numerical solutions for $\gamma(\alpha; \Lambda, h)$ are given in Fig. 3. The data have been computed for $h = 3$ (e.g. $V_\infty = 28.5$ Kft/sec in pure oxygen and $\alpha_\infty = 0$). The temperature exponent s in Eqs. (26) is set equal to zero as suggested by recent experimental results.[23] A large range of values of Λ is considered, so as to explore the parametric dependence of the solution. When the following values are substituted into Eqs. (19) and (24)

$$\delta = 3.5\ \text{Å} \qquad \Omega^{2,2} = 0.7 \qquad W_o = 32 \qquad Sc = 1$$
$$C = 6 \times 10^{14}\ \text{cm}^3\,\text{gm}^{-1}\,\text{sec}^{-1} \qquad T_d = 6 \times 10^4\ ^\circ\text{K} \qquad (34)$$

one finds

$$\Lambda = 82 \tag{35}$$

Actually, the choice of C in Eqs. (34) corresponds to O_2 dissociation in a bath of Argon.[23] By analogy with the lower temperature case,[24] it is expected that O-atoms would have a higher collision efficiency than Argon, so that Eq. (35) may give a lower limit for Λ .

The dashed lines in Fig. 3 represent the inviscid solution, Eq. (28), and the dotted lines define the solution for pure diffusion, Eq. (9). The exact solutions including diffusion and relaxation effects are shown as full lines. Figure 3 demonstrates that diffusion is quite effective in smoothing out the concentration gradients, i.e., for a given $\Lambda \geq 10$, the exact solution is much smaller than the inviscid solution. In fact, $\mathcal{Y}$ is a weak function of Λ for $\Lambda \geq 10^2$ so that the solution is essentially that obtained for strong diffusion (see Eq. (29) and the subsequent discussion). On the other hand, the dashed and full curves in Fig. 3 agree comparatively well at $\Lambda = 1$, indicating that $\Lambda = 1$ defines a lower limit of the diffusion-controlled regime.

For the cases considered in Fig. 3, one finds appreciable concentrations immediately behind the translation zone, e.g.

$$\begin{aligned} \alpha_{SH} &= 0.17 \qquad \text{for} \quad \Lambda = 1 \\ \alpha_{SH} &= 0.46 \qquad \text{for} \quad \Lambda = 10 \end{aligned} \tag{36}$$

Thus, diffusion creates finite atom concentrations immediately behind the translation zone. This behavior is analyzed in Ref. 14 for a fully viscous shock layer with a cold wall. The present results show that species diffusion has a similar effect on normal-shock flows which do not involve heat losses.

The effect of finite concentrations at the shock on the concentration profiles is apparent from the full curves of Fig. 4. The curves are plotted against the scaled coordinate, $\sigma' \sqrt{\Lambda}$, for Λ = 1, 10 and 10^2 and h = 3.0 (same as in Fig. 3). The dashed curves represent the inviscid solutions. The solutions including diffusion and conduction are expressed in the form

$$\mathcal{J}(\alpha;\Lambda,h) - \mathcal{J}(\alpha_{SH};\Lambda,h) = \sigma'\sqrt{\Lambda} = \sum \tag{37}$$

where

$$\mathcal{J}(\alpha;\Lambda,h) = \int_0^{\alpha} \frac{d\alpha}{z(\alpha;\Lambda,h)} \tag{38}$$

In other words, the profiles $\alpha(\sum)$ are obtained by cutting off the basic profile

$$\mathcal{J}(\alpha;\Lambda,h) = \sum$$

at $\alpha \leq \alpha_{SH}$. This procedure should be compared to that applied in Ref. 1 to account for the effect of free-stream dissociation on inviscid flows.

For Λ = 1, it is found that the function $\mathcal{J}$ agrees essentially with the inviscid solution $\mathcal{J}(\alpha, 0, h)$. Consequently the diffusion profile can be obtained by cutting off the inviscid solution at $\alpha \leq \alpha_{SH}$. When diffusion is weak, it modifies the inviscid flow in the same manner as the presence of a finite atom concentration in the free stream. The strong effect of diffusion is apparent for Λ = 10 and 10^2. For fixed α , the comparison with the inviscid profiles shows that the concentration gradient is strongly reduced by diffusion. For a fixed distance behind the transport shock, the dissociation fraction is, in general, strongly increased. However, the relaxation length for the variable $\sigma'\sqrt{\Lambda}$ is not drastically modified by diffusion. Hence, the relaxation length can be estimated for practical purposes on the basis of the inviscid solution for the

same value of Λ . Thus, the determination of the rate coefficient from a measurement of the relaxation time is not critically affected by species diffusion.

The above results for a Lighthill gas agree essentially with those obtained from the linearized theory of Section II. The only difference is that species diffusion and heat conduction have a stronger effect on profile shape in the nonlinear theory.

Effects of Diffusion for Airflows

Strong shock waves in air are briefly studied in Appendix B. The example chosen is a shock of 23 Kft/sec. Then, the oxygen-atom and temperature profiles are not modified by diffusion but the nitric oxide and electron profiles are strongly affected (see Figs. (B-1) and (B-2). For instance, the nitric oxide and electron concentrations immediately behind the translation zone are raised to 2.5×10^{-3} and 10^{-5} moles per original mole respectively, due to upstream diffusion from the relaxation zone. These results are based on an approximate solution and it is clear that further work is required.

3.4 Effect of Ambient Dissociation

Introduction

The following analysis is concerned with the effect of free-stream dissociation (ambient dissociation) on nonequilibrium flows in strong shocks, when species diffusion and heat conduction are included.

Ambient dissociation is involved in several applications of hypersonic flow (cf. Ref. 1). For instance, high-enthalpy wind tunnels provide test flows with finite atom concentrations. In the following discussion, nonequilibrium flows with and without ambient dissociation will be called tunnel and flight solutions,

respectively. This convenient terminology is borrowed from Ref. 1. It is not meant to imply a basic difference between tunnel experiments and flight.

The effect of ambient dissociation on inviscid nonequilibrium flows is studied in Ref. 1. There, a subtraction rule was established, giving a flight solution by subtraction of the ambient dissociation fraction from a tunnel solution. The correlated flows have equal shock speeds.

The subtraction rule is now extended to flows involving species diffusion. The analysis is given for a Lighthill gas with the same assumptions as in Section 3.1 (normal shock flow, constant pressure and enthalpy, viscosity varying as $\sqrt{T}$).

General Subtraction Rule

For the present application, one requires a more general statement of the subtraction rule than is available in Ref. 1. Consider a rate equation of the form

$$\frac{d\alpha}{dx} = P(\alpha)\,\Phi(T), \qquad T = d(h-\alpha) \tag{39}$$

where h is the enthalpy parameter (see Eq. (22)) and d is assumed constant.* Furthermore $P(\alpha)$ varies slowly with α whereas $\Phi(T)$ is a strong function of the temperature (cf $F(\alpha,h)$ in Eqs. (26)). The boundary condition for Eq. (39) is prescribed at the shock

$$x = 0 \;:\; \alpha = \alpha_{SH} \tag{40}$$

The general subtraction rule relates two solutions for instance $\alpha_1(x)$ and

---

* As seen from Eqs. (21), the actual variation of $d(\alpha)$ is small. It can be included at the cost of a minor complication (see Ref. 1).

$\alpha_2(x)$, corresponding to the enthalpies h_1 , h_2 and to the shock values $\alpha_{1,SH}$, $\alpha_{2,SH}$ respectively. Then

$$\alpha_1(x;\alpha_{1,SH},h_1) - \alpha_{1,SH} \approx \alpha_2(\eta_{12}x;\alpha_{2,SH},h_2) - \alpha_{2,SH} \qquad (41)$$

$$T(x;\alpha_{1,SH},h_1) \approx T(\eta_{12}x;\alpha_{2,SH},h_2)$$

with the conditions

$$h_1 - \alpha_{1,SH} = h_2 - \alpha_{2,SH}, \qquad \eta_{12} = \frac{P(\alpha_{1,SH})}{P(\alpha_{2,SH})} \qquad (42)$$

Equations (41) and (42) are proved in the same manner as in Ref. 1. The situation considered in Ref. 1 corresponds to

$$\alpha_{1,SH} = \alpha_\infty , \qquad \alpha_{2,SH} = \bar{\alpha}_{SH} = 0 \qquad (43)$$

i.e. to inviscid tunnel and flight ($\alpha_\infty = 0$) solutions respectively. The flight solution is denoted by barred symbols. In the present case, this distinction loses its mathematical significance because species diffusion creates a finite α_{SH} whatever the value of α_∞ . However, the notation will be retained for convenience. The concentrations at the shock are now determined by Eqs. (27). Applying Eqs. (41) with $x = \sigma'$,

$$\alpha_{SH} - \alpha_\infty = \frac{d\alpha}{d\sigma'}$$

$$\bar{\alpha}_{SH} = \frac{P(\bar{\alpha}_{SH})}{P(\alpha_{SH})}\frac{d\alpha}{d\sigma'} \qquad (44)$$

Thus, α_{SH} , $\bar{\alpha}_{SH}$ and α_∞ are related by an equation independent of $\Phi(T)$, namely

$$\frac{\alpha_{SH} - \alpha_\infty}{\bar{\alpha}_{SH}} = \frac{P(\alpha_{SH})}{P(\bar{\alpha}_{SH})} \qquad (45)$$

The cases of weak and strong diffusion will now be treated separately.

Weak Diffusion

The principal effect of diffusion for small values of Λ is to establish a finite concentration at the shock, as shown in Section 3.3. Hence, the

appropriate rate equation has the form of Eqs. (39). The results of Ref. 1 can be applied directly. Referring to Eq. (23), one has

$$P(\alpha) = \frac{1-\alpha}{(1+\alpha)^2}(h - \alpha_\infty) \tag{46}$$

Thus, Eqs. (41), (42) and (45) become

$$\alpha(\sigma'; h) - \alpha_{SH} \approx \bar{\alpha}(a\sigma'; \bar{h}) - \bar{\alpha}_{SH}$$

$$T(\sigma'; h) \approx \bar{T}(a\sigma'; \bar{h}), \qquad \frac{\alpha_{SH} - \alpha_\infty}{\bar{\alpha}_{SH}} = a \tag{47}$$

where

$$a = \frac{1-\alpha_{SH}}{1-\bar{\alpha}_{SH}} \frac{(1+\bar{\alpha}_{SH})^2}{(1+\alpha_{SH})^2} \frac{h-\alpha_\infty}{\bar{h}}, \qquad h - \alpha_{SH} = \bar{h} - \bar{\alpha}_{SH} \tag{48}$$

Equations (47) are verified by the examples given in Fig. 5. The subtracted concentrations, $\alpha - \alpha_{SH}$ and $\bar{\alpha} - \bar{\alpha}_{SH}$ are plotted against the dimensionless distance behind the shock $\frac{\sigma}{\ell}$ which is defined in Eqs. (33). In terms of the physical coordinate $\frac{\sigma}{\ell}$, the scaling factor a in Eqs. (47) is replaced by $\frac{1-\bar{\alpha}_{SH}}{1-\alpha_{SH}} \frac{(1+\alpha_{SH})^2}{(1+\bar{\alpha}_{SH})^2}$. The full curve in Fig. 5 corresponds to a flight solution for $\bar{\Lambda} = 1$ and $\bar{h} = 3.0$. The triangles and ellipses correspond to the values of α_∞ defined in the table at the left and the values of α_{SH} for various α_∞ are deduced from the analysis of Section 3.3. The enthalpies for $\alpha_\infty = 0.13$ and 0.27 are $h = 3.1$ and $h = 3.2$ respectively. The correlation obtained by applying the above scaling factor is found to be very good. This is not surprising in view of the inviscid character of the concentration profile for $\Lambda = 1$ and of the accuracy of the subtraction rule[1] for inviscid flow.

Strong Diffusion

In the limit of strong diffusion, the subtraction rule is justified by the following analogy between inviscid and strongly diffused flows. For large Λ the

analytic solution, Eqs. (32), reduces to

$$\frac{1}{\sqrt{\Lambda}} \frac{d\alpha}{d\sigma'} \approx (1-\alpha) \sqrt{F \alpha, h}$$

or

$$\frac{d\alpha}{d\sigma'} \approx \sqrt{\Lambda} \frac{1-\alpha}{1+\alpha} T'^{-\frac{2s+3}{4}} \exp\left(-\frac{1}{2T'}\right) \tag{49}$$

Equation (49) has the same form as Eq. (39). Thus, the strongly diffused profile obeys a relaxation equation of inviscid type and the subtraction rule is still directly applicable.

To be applicable to strong diffusion, Eqs. (47) and (48) need only be changed by a new definition of the scaling factor

$$a = \frac{1-\alpha_{SH}}{1-\bar{\alpha}_{SH}} \frac{1+\bar{\alpha}_{SH}}{1+\alpha_{SH}} \left(\frac{h-\alpha_\infty}{\bar{h}}\right)^{1/2} \tag{50}$$

since $(1+\alpha)^2$ and $(h-\alpha_\infty)$ are replaced in Eq. (46) by $(1+\alpha)$ and $\sqrt{h-\alpha_\infty}$ respectively.

The correlation for strong diffusion is examined in Fig. 5. The dashed curve is a flight solution ($\bar{\Lambda} = 10$, $\bar{h} = 3.0$) and the squares and circles denote the values of α_∞ defined in the table at the right. The corresponding enthalpies are $h = 3.1$ and 3.2 as for the case $\Lambda = 1$. The values of α_{SH} are much higher than for $\Lambda = 1$, reflecting an increased effect of diffusion. The scaling factor applied to $\frac{\sigma}{l}$ is found to be $\frac{1-\alpha_{SH}}{1-\bar{\alpha}_{SH}} \frac{1+\bar{\alpha}_{SH}}{1+\alpha_{SH}} \left(\frac{\bar{h}}{h-\alpha_\infty}\right)^{1/2}$ from Eqs. (33) and (50). The correlation is satisfactory. The squares and circles at the right correspond to the theoretical limit of validity of the subtraction rule derived in Ref. 1, namely

$$\bar{\alpha} - \bar{\alpha}_{SH} = 1 - \alpha_{SH}$$

Even in this limit, the error of the subtraction rule does not exceed 10%.

In summary, the subtraction rule of Ref. 1 has been extended to normal shock flows with species diffusion. Then, the concentration at the shock must be subtracted.

Furthermore, it is shown that the concentrations at the shock for tunnel and flight solutions (dissociated and undissociated free streams) are related independently of the rate coefficient.

IV. CONCLUDING REMARKS

The report considers the effect of species diffusion and heat conduction on nonequilibrium gas flows behind strong shocks. In the present flow model, the shock wave is divided in two zones which are controlled by translational equilibration and relaxation processes respectively. Within the translation zone, the gas achieves a high enthalpy by translational equilibration through elastic collisions without appreciable internal excitation. Within the relaxation zone, inelastic collisions bring about internal excitation subject to species diffusion and heat conduction. The upstream boundary of the relaxation zone is determined by matching the concentration profile for the relaxation zone with the pure diffusion solution applicable within the translation zone.

The analysis is developed for two chemical models, vibrational relaxation and dissociation. Applications to air flows with coupled chemistry are indicated. The results show important effects of species diffusion and heat conduction at shock speeds above 20 Kft/sec. Species diffusion and heat conduction strongly decrease the concentration gradients predicted by inviscid solutions for the relaxation zone. Furthermore, finite concentrations of excited species diffuse into the translation zone. On the other hand, the relaxation length is not appreciably modified.

The extent of the effects depends on the relaxation process. Vibrational relaxation is rather insensitive to heat conduction because of the small energy content involved and of the weak dependence of relaxation time on translational temperature. However, the diffusion of vibrationally excited molecules is a major effect at shock speeds as low as 20 Kft/sec. Thus the vibrational temperature immediately behind the translation zone in pure O_2 at 20 Kft/sec (see Fig. 2)

is found to be 4000°K when we include diffusion. The inviscid solution however predicts a vibrational temperature equal to the free stream value, namely 300°K in the present example.

At 23 Kft/sec in air, electron and nitric oxide distributions are strongly affected by diffusion; atom and temperature distributions are not. Again, high molar concentrations are created immediately behind the translation zone, i.e. 10^{-5} moles per original mole for electrons and 2.5×10^{-3} for nitric oxide. Finally, at 29 Kft/sec, the dissociation of pure O_2 is shown to be markedly influenced by both diffusion and conduction. Analytic and numerical solutions are given and the effect of changing the rate coefficient is examined. A ten-fold decrease of the rate coefficient from the presently used value does not materially reduce the importance of transport processes.

The subtraction rule of Ref. 1 for a dissociated free stream is extended to nonequilibrium flows involving species diffusion and heat conduction. In most cases, the effect of free stream dissociation on an inviscid flow is quite similar to that of transport processes. The analogy requires that the state of the gas be the same immediately behind the translation zone. Thus, the shock speed must be fixed and the free stream dissociation must equal that created by species diffusion.

The full validity of the present results will become clearer with our increasing knowledge of high-temperature air chemistry. However, it is suggested that species diffusion and heat conduction should not be routinely neglected in the study of relaxation zones behind strong shocks. These effects should also play an important role in blunt-body flows near the bow shock even when the Reynolds number based on body radius is large.

APPENDIX A: ANALYSIS OF VIBRATIONAL RELAXATION

In this Appendix, the relaxation equation for vibration is derived, to include the diffusion of excited molecules by elastic collisions. A simple approximation for the vibrational energy is applied to obtain solutions of the inviscid relaxation equation. These solutions are used to justify the linearized theory of Section 2.3.

A.1 Rate Equation

The population y_n of the n^{th} quantum level satisfies the following relaxation equation[16]

$$\rho \frac{dy_n}{d\sigma} = \left(k_{n-1,n}\, y_{n-1} + k_{n+1,n}\, y_{n+1}\right) - \left(k_{n,n-1} + k_{n,n+1}\right) y_n + \frac{1}{\rho} \frac{d}{d\sigma}\left(\mu \frac{dy_n}{d\sigma}\right) \tag{A-1}$$

where the convection rate, $\rho \frac{dy_n}{d\sigma}$, is balanced by the effect of inelastic collisions (first two brackets) and by the diffusion rate due to elastic collisions. Oscillator transitions are taken to occur between adjacent levels with probabilities k_{mn} $(m \longrightarrow n)$ in accordance with the simple harmonic oscillation theory of Ref. 18. The diffusion term is given for a Schmidt number equal to unity (cf. Eq. (3)) and the viscosity coefficient, μ, is assumed independent of the y_n's. The correlation between vibrational and translational energy is neglected so that μ is also independent of n.

A straightforward application of the method of Ref. 18 leads to

$$\rho \frac{d\epsilon}{d\sigma} - \frac{1}{\rho} \frac{d}{d\sigma}\left(\mu \frac{d\epsilon}{d\sigma}\right) = \frac{\tilde{\epsilon} - \epsilon}{\tau} \tag{A-2}$$

In Eq. (A-2), the energies ϵ and $\tilde{\epsilon}$ and the relaxation time τ are defined by

$$\epsilon = \sum_{n=1}^{\infty} n y_n = \psi\left(\frac{T_v}{\theta_v}\right), \qquad \tilde{\epsilon} = \psi\left(\frac{T}{\theta_v}\right)$$

$$\psi(x) = \left(e^{1/x} - 1\right)^{-1}, \qquad \frac{1}{\tau} = k_{10}\left(1 - e^{-\frac{\theta_v}{T}}\right)^{-1} \tag{A-3}$$

where θ_v is the characteristic temperature of vibration for the given gas and T_v and T are the local vibrational and translational temperatures. Equation (A-2) differs from the rate equation given in Ref. 18 only by the inclusion of the diffusion term.

A.2 An Approximation for the Vibrational Energy

For the analysis of Eq. (A-2), it is useful to note a simple approximation of the energy function ψ, namely

$$\psi(x) \approx x - 0.4 \tag{A-4}$$

The accuracy of Eq. (A-4) is demonstrated in Fig. (A-1) where the full and dashed curves represent the exact and approximate values for $\psi(x)$ respectively. The agreement is excellent for $x \geq 0.6$. Thus, both ϵ and $\tilde{\epsilon}$ are given by

$$\epsilon = \frac{T_v}{\theta_v} - 0.4, \qquad \tilde{\epsilon} = \frac{T}{\theta_v} - 0.4 \tag{A-5}$$

for T_v or $T \geq 0.6\ \theta_v$. This is a wide range of validity since $0.6\ \theta_v$ is generally a low temperature (1400°K for pure O_2).

At high temperatures, Eqs. (A-5) agree with the classical limit

$$\epsilon = \frac{T_v}{\theta_v}, \qquad \tilde{\epsilon} = \frac{T}{\theta_v} \tag{A-6}$$

However, Eqs. (A-6) are inaccurate below 7000°K where Ref. 15 suggests the assumption of half-excited vibration. On the other hand, Eqs. (A-5) remain accurate for higher temperatures than the formulation of Ref. 15. When energy differences are of interest, say $\epsilon(T_1) - \epsilon(T_2)$, it is clear that Eqs. (A-5) and

(A-6) are equivalent. This situation arises in Ref. 3 for the quasi-equilibrium range of coupled vibration-dissociation of O_2. Then, the classical assumption of Eqs. (A-6) can be used accurately at temperatures T_1 and T_2 well below 7000°K. Anharmonicity and dissociation cutoff are found to be the more important causes of error.[3]

A.3 Exact Inviscid Solutions Behind a Normal Shock.

Verification of Linearized Theory.

Behind the shock, the pressure change due to vibrational relaxation cannot exceed 5%. Hence, it is justified to set

$$p \approx \frac{5}{6} \rho_\infty V_\infty^2 \tag{A-7}$$

Applying Eqs. (A-5), (A-7) and the continuity and state equations, the inviscid rate equation reduces to

$$\frac{3}{5} \frac{V_\infty T'}{h} \frac{d T_v'}{d\sigma} = \frac{T' - T_v'}{\varphi(T')} \tag{A-8}$$

where the following definitions have been introduced

$$T' = \frac{T}{\theta_v}, \qquad T_v' = \frac{T_v}{\theta_v}, \qquad \tau = \frac{\varphi(T')}{p}, \qquad h = \frac{W_0 V_\infty^2}{2 \mathcal{R} \theta_v} \tag{A-9}$$

The enthalpy equation gives

$$T' = \frac{2}{7}\left(h + 0.4 - T_v'\right) \tag{A-10}$$

Equation (A-8) is now solved explicitly in the form

$$\frac{155}{18} \frac{\rho_\infty V_\infty \sigma}{\varphi(\beta = 0, h)} = \xi = \int_0^\beta \frac{h + 0.4\beta}{h} \frac{1}{\left(1 + \frac{2}{7}\beta\right)^2} \frac{\varphi(\beta, h)}{\varphi(0, h)} \frac{d\beta}{1 - \beta} \tag{A-11}$$

where β is the variable defined in Eq. (6)

$$\beta = \frac{\epsilon}{\tilde{\epsilon}} = \frac{T_v' - 0.4}{T' - 0.4} \tag{A-12}$$

Here, ϵ is assumed to vanish at the shock (cold free stream). This corresponds to $T'_{v,sh} = 0.4$ in the application of Eqs. (A-5). The error involved in using Eqs. (A-5) for such low values of T_v' is not critical for the present purpose.

Note the significance of the various factors in the integral of Eq. (A-11). Under most conditions of interest, h is sufficiently high that $\frac{h + 0.4\beta}{h}$ can be set equal to one. The factor $\frac{1}{(1+\frac{2}{7}\beta)^2}$ arises directly from the energy balance, Eq. (A-10), whereas $\varphi(\beta, h)$ as defined in Eq. (A-9) expresses the variation of relaxation time. For inviscid flow, the linearized theory of Section 2.3 sets both $\frac{1}{(1+\frac{2}{7}\beta)^2}$ and $\frac{\varphi(\beta,h)}{\varphi(0,h)}$ equal to one, giving

$$\beta = 1 - e^{\xi} \tag{A-13}$$

The validity of this solution is established in Fig. (A-2) where $h = 20$ for pure O_2 (shock Mach number of 16). The circles represent Eq. (A-13) which is found to agree very well with the exact solution of Eq. (A-11) (full curve). The dashed curve of Fig. (A-2) is obtained by taking $\frac{\varphi(\beta,h)}{\varphi(0,h)}$ equal to one in Eq. (A-11). This curve demonstrates the effect of varying q and $\tilde{\epsilon}$. Since φ increases with distance behind the shock, the dashed curve predicts a higher value for β than the exact solution at fixed ξ. On the other hand, $(1+\frac{2}{7}\beta)^{-2}$ decreases with increasing ξ. Thus, the approximation $(1+\frac{2}{7}\beta)^{-2} \approx 1$ has an effect opposite to that of assuming constant φ. In the example of Fig. (A-2), the two errors are found to cancel. For a more general case including diffusion, the interplay of the various approximations is similar and an equally good accuracy of the linearized theory is expected.

APPENDIX B: SPECIES DIFFUSION IN AIRFLOWS

The chemical relaxation zone behind strong shocks in air is governed by a coupled system of reactions,[24] including oxygen and nitrogen dissociation, nitric oxide shuffle reactions and various ionization and charge exchange reactions.[8] Numerical solutions have been obtained[8, 25] under the assumption that transport processes can be neglected in the relaxation zone. The results of this Appendix suggest that transport processes can cause an appreciable increase in nitric oxide and electron concentrations near the shock for a shock speed as low as 23 Kft/sec. For simplicity, vibrational equilibrium is assumed.

At lunar reentry speed, all chemical species display extreme concentration gradients in the inviscid solution.[8] At 23 Kft/sec, diffusion and heat conduction can be shown to have little effect on atom and temperature distributions. However, nitric oxide and electron distributions are strongly modified. At a lower speed, 15 Kft/sec, the transport processes are unimportant for all species.

B.1 Assumptions

The reactions controlling nitric oxide and electron production are taken to be

$$\begin{aligned} O + N_2 &\rightleftharpoons NO + N \\ N + O &\rightleftharpoons NO^+ + e^- \\ N + O_2 &\rightleftharpoons NO + O \\ NO + M &\rightleftharpoons N + O + M \end{aligned} \qquad \text{(B-1)}$$

where M is any collision partner. The reaction rates are the same as in Ref. 25. An exact solution including diffusion and heat conduction is difficult to obtain in view of the high order of the nonlinear system of differential equations. However, an approximate solution is easily found as follows.

It is assumed that the transport processes do not affect net rates of NO and e^- production, as functions of position. The justification is based on properties of the inviscid solution[25] for 23 Kft/sec shock speed. Near the shock, the forward rates of reactions (B-1) are strongly dominant (See Fig. 13 of Ref. 25). Actually, the last two reactions are not important because of low N and NO concentrations. In addition, these reactions tend to cancel each other. As a result, the net rates for NO and e^- show no explicit dependence on NO and e^- concentrations. The implicit dependence introduced by the enthalpy and species conservation equations is weak ((NO) and $(e^-) \ll 1$). Similarly, the N concentration is uncoupled from (NO) and (e^-). Thus, the net rates of NO and e^- production are controlled by (O), (O_2) and (N_2). These species do not have large enough concentration gradients to be affected by diffusion and the basic assumption appears justified near the shock.

Far from the shock, all species have small gradients (approach to equilibrium) and diffusion is unimportant. Hence, the net rates are still given by the inviscid solution.

In the present analysis, electron diffusion is assumed to be ambipolar, in view of the electron concentrations involved. This gives a conservative estimate of diffusion effects. In addition, the product $\rho\mu$ is kept constant for NO and e^- and equal to the value at the shock for inviscid flow. The Schmidt number is one and pressure variations are still neglected in the relaxation zone.

B. 2 Approximate Solution

The rate equation for nitric oxide or electrons can be written

$$\frac{d\gamma_d}{d\eta} - \delta \frac{d^2\gamma_d}{d\eta^2} = \frac{d\gamma_i}{d\eta} \qquad \text{(B-2)}$$

by applying the above assumptions. In Eq. (B-2), γ represents moles per original mole; γ_i and γ_d are the solutions for inviscid flow and for diffusive flow respectively. The coefficient δ is a diffusion constant equal to $D'\mu_{SH}\left(\frac{\rho_{SH}}{\rho_\infty} - 1\right)$ where SH denotes conditions at the shock for inviscid flow. The variable η is defined for airflows in Ref. 26, namely

$$\eta = D' \int_0^\sigma \frac{p\, d\sigma}{g}, \qquad D' = 1 \frac{\text{cm-sec}}{\text{gm}} \qquad \text{(B-3)}$$

with $\sigma = 0$ at the shock for inviscid flow. It has been shown that η can be used to map inviscid shock relaxation zones onto streamlines of Newtonian flows. When $\rho\mu$ is constant in a one-dimensional flow, η becomes proportional to the variable σ' of Eq. (6).

Equation (B-2) expresses the balance between convection $\frac{d\gamma_d}{d\eta}$, diffusion $\left(\delta \frac{d^2\gamma_d}{d\eta}\right)$ and net rate of production approximated by the inviscid value $\frac{d\gamma_i}{d\eta}$. The equation is readily integrated to give

$$\gamma_d - \delta \frac{d\gamma_d}{d\eta} = \gamma_i \qquad \text{(B-4)}$$

which satisfies the boundary condition at infinity

$$\eta = +\infty : \gamma_d = \gamma_i = \text{equilibrium level} \qquad \text{(B-5)}$$

A further integration yields a closed form solution

$$\gamma_d = \frac{1}{\delta} e^{\frac{\eta}{\delta}} \int_\eta^\infty e^{-\frac{\eta'}{\delta}} \gamma_i(\eta')\, d\eta' \qquad \text{(B-6)}$$

Other solutions of Eq. (B-4) contradict the above boundary condition. Finally, the value of γ_d at the shock must satisfy

$$\gamma_d - \delta \frac{d\gamma_d}{d\eta} = 0 \qquad \text{(b}$$

by analogy with the first Eq. (10) (Set $\beta = \gamma_d$, $\beta_\infty = 0$). This condition agrees with Eq. (B-4) only when $\gamma_i(\eta)$ vanishes, i.e., at the location of the shock for the inviscid solution ($\eta = \sigma' = 0$).

B.3 Discussion of the Results

Equation (B-6) is easily computed from the given inviscid solution, $\gamma_i(\eta)$. The results are shown in Figs. 8 and 9 for nitric oxide and electrons respectively at a shock speed of 23 Kft/sec. For $\eta > 0.1$, diffusion has practically no effect. In particular, the locations and magnitudes of the NO and e^- maxima are unchanged. Closer to the shock, the profiles are strongly modified. High concentrations are found at the shock, namely 2.5×10^{-3} and 10^{-5} moles per original mole for NO and e^- respectively.

The validity of the above results is not yet clear in view of the assumptions required for the solution. These assumptions are based on the behavior of the inviscid solution; they may become invalid when diffusion is important. In particular, the last reaction (B-1) may prove to be a strong consumer of nitric oxide at the high temperatures near the translation zone.

REFERENCES

1. Gibson, W. E., The Effect of Ambient Dissociation and Species Diffusion on Nonequilibrium Shock Layers. IAS Preprint 63-70, presented at the IAS Meeting of January 1963.
2. Talbot, L., Survey of the Shock Structure Problem. ARS Journal, Vol. 32, p. 1009, July 1962.
3. Treanor, C. E., Vibrational Relaxation Effects in Dissociation Rate-Constant Measurements. CAL Rept. AG-1729-A-1, August 1962.
4. Parker, J. G., Rotational and Vibrational Relaxation in Diatomic Gases. The Physics of Fluids, Vol. 2, p. 449, February 1959.
5. Gaitatzes, G. and Bloom, M. H., On the Interior of Normal Shocks According to Continuum Theory, Including Rate Thermochemistry. Polytechnic Institute of Brooklyn, ARL Report 65, June 1961.
6. Scala, S. M. and Talbot, L., Shock Wave Structure with Rotational and Vibrational Relaxation. G. E. Report, AFOSR 1494, R62SD32, October 1962.
7. Talbot, L. and Scala, S. M., Shock Wave Structure in a Relaxing Diatomic Gas. Rarefied Gas Dynamics, edited by L. Talbot, p. 603, Academic Press, New York, 1961.
8. Eschenroeder, A. Q., Daiber, J. W., Golian, T. C. and Hertzberg, A., Shock Tunnel Studies of High Enthalpy Ionized Airflows. Presented at AGARD Meeting on High Temperature Aspects of Fluid Dynamics, Brussels, Belgium, March 1962.
9. Weymann, H. D., Electron Diffusion Ahead of Shock Waves in Argon. Maryland U., Inst. for Fluid Dyn. and App. Math., Tech. Note No. BN-197, AFOSR-TN-60-334, March 1960.

10. Wetzel, L., Precursor Effects and Electron Diffusion from a Shock Front. The Physics of Fluids, Vol. 5, p. 824, June 1962.

11. Sherman, F.S., Shock-Wave Structure in Binary Mixtures of Chemically Inert Perfect Gases. Jour. Fluid Mech., Vol. 8, p. 465, July 1960.

12. Lees, L., Convective Heat Transfer with Mass Addition and Chemical Reactions. Third AGARD Combustion and Propulsion Panel Colloquium, Palermo, March 1958.

13. Cheng, H.K., Hypersonic Shock-Layer Theory of the Stagnation Region at Low Reynolds Number. Proc. Heat Transfer and Fluid Mechanics Inst., Univ. of Southern California, Stanford Univ. Press, p. 161, June 1961.

14. Cheng, H.K., The Blunt-Body Problem in Hypersonic Flow at Low Reynolds Number. IAS Preprint 63-92, presented at the IAS Meeting of January 1963.

15. Lighthill, M.J., Dynamics of a Dissociating Gas, Part I. Equilibrium Flow. J. Fluid Mech., Vol. 2, p. 1, January 1957.

16. Penner, S.S., Introduction to the Study of Chemical Reactions in Flow Systems. Butterworths Scientific Publications, London, 1955.

17. Gibson, W.E. and Moore, F.K., Acoustic Propagation in a Diatomic Gas Subject to Thermal or Chemical Relaxation. CAL Rept. HF-1056-A-2, October 1958.

18. Landau, L.D. and Teller, E., Contribution to the Theory of Sound Dispersion. Physik. Z. Sowjetunion, 10, 34, 1936.

19. Blackman, V.H., Vibrational Relaxation in Oxygen and Nitrogen. J. Fluid Mech., Vol. 1, pp. 61-85 (1956).

20. Camac, M., O_2 Vibration Relaxation in Oxygen-Argon Mixtures. J. Chem. Phys., Vol. 34, No. 2, pp. 460-470, February 1961.

21. Moore, F.K., On the Viscosity of Dissociated Air. ARS Jour., Tech. Note, Vol. 32, p. 1415, September 1962.

22. Gibson, W.E., Dissociation Scaling for Nonequilibrium Blunt-Nose Flows. ARS Jour., Vol. 32, No. 2, p. 285, February 1962.

23. Wray, K.L., Shock-Tube Study of the O_2-Ar Rates of Dissociation and Vibrational Relaxation. Jour. Chem. Phys., Vol. 37, p. 1254, September 1962.

24. Wray, K.L., Chemical Kinetics of High Temperature Air. Hypersonic Flow Research, edited by F. R. Riddell, ARS, p. 181, 1961.

25. Hall, J.G., Eschenroeder, A.Q. and Marrone, P.V., Blunt-Nose Inviscid Airflows with Coupled Nonequilibrium Processes. J. Aero/Space Sci., Vol. 29, No. 9, p. 1038, 1962.

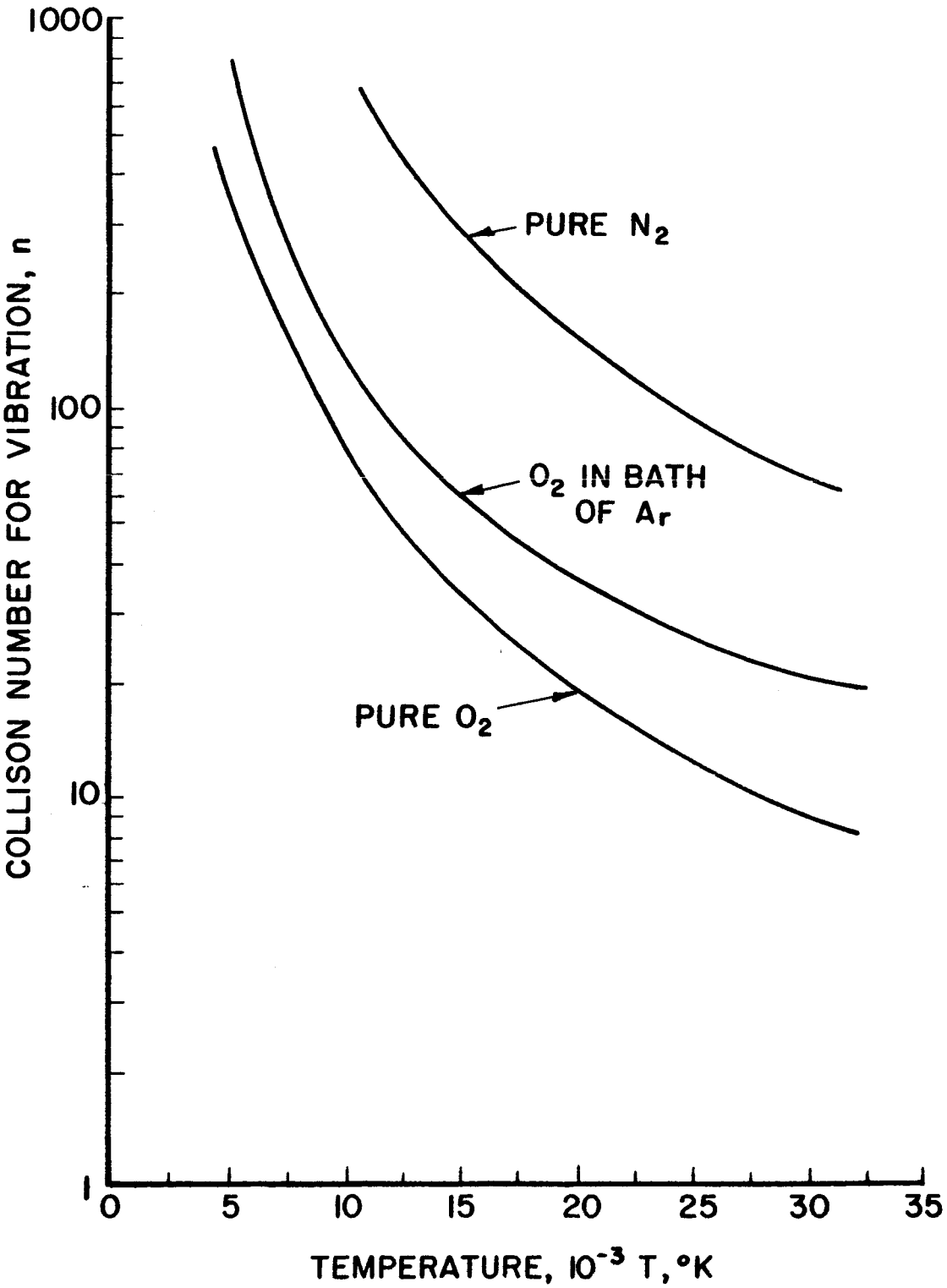

Figure I COLLISION NUMBER FOR VIBRATION

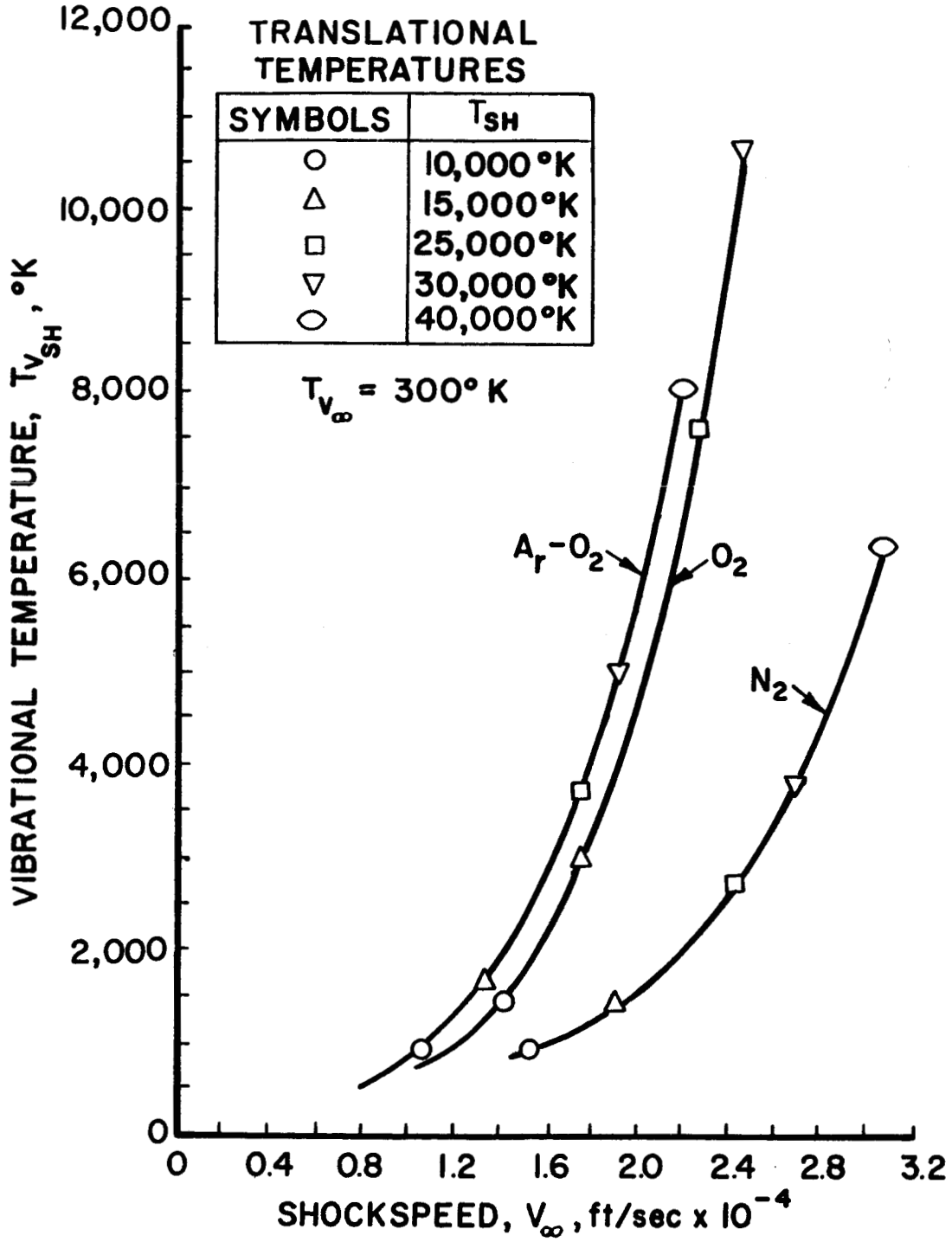

Figure 2 VIBRATIONAL TEMPERATURE BEHIND TRANSLATION ZONE

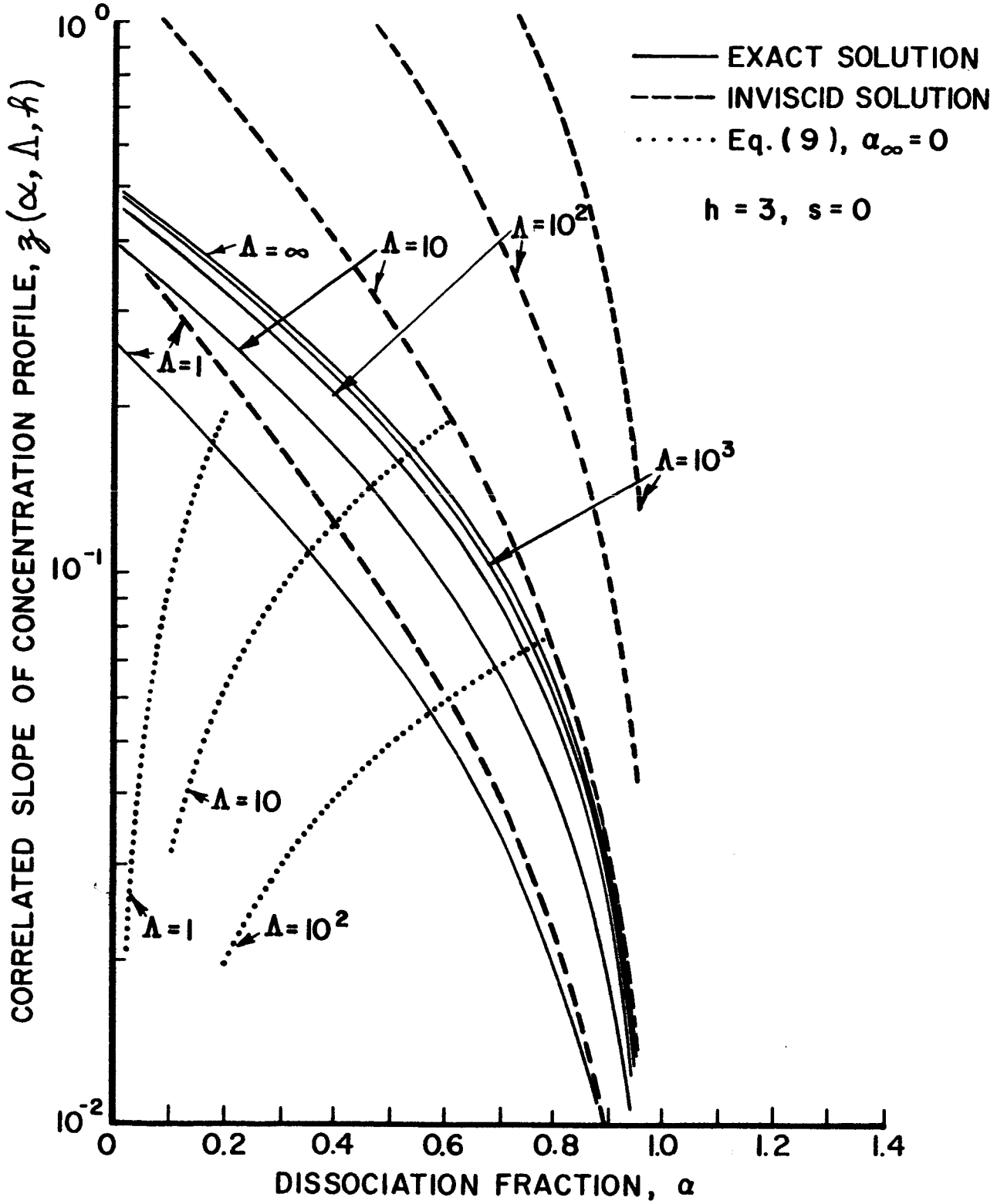

Figure 3 EFFECT OF DIFFUSION ON CONCENTRATION GRADIENTS FOR A LIGHTHILL GAS

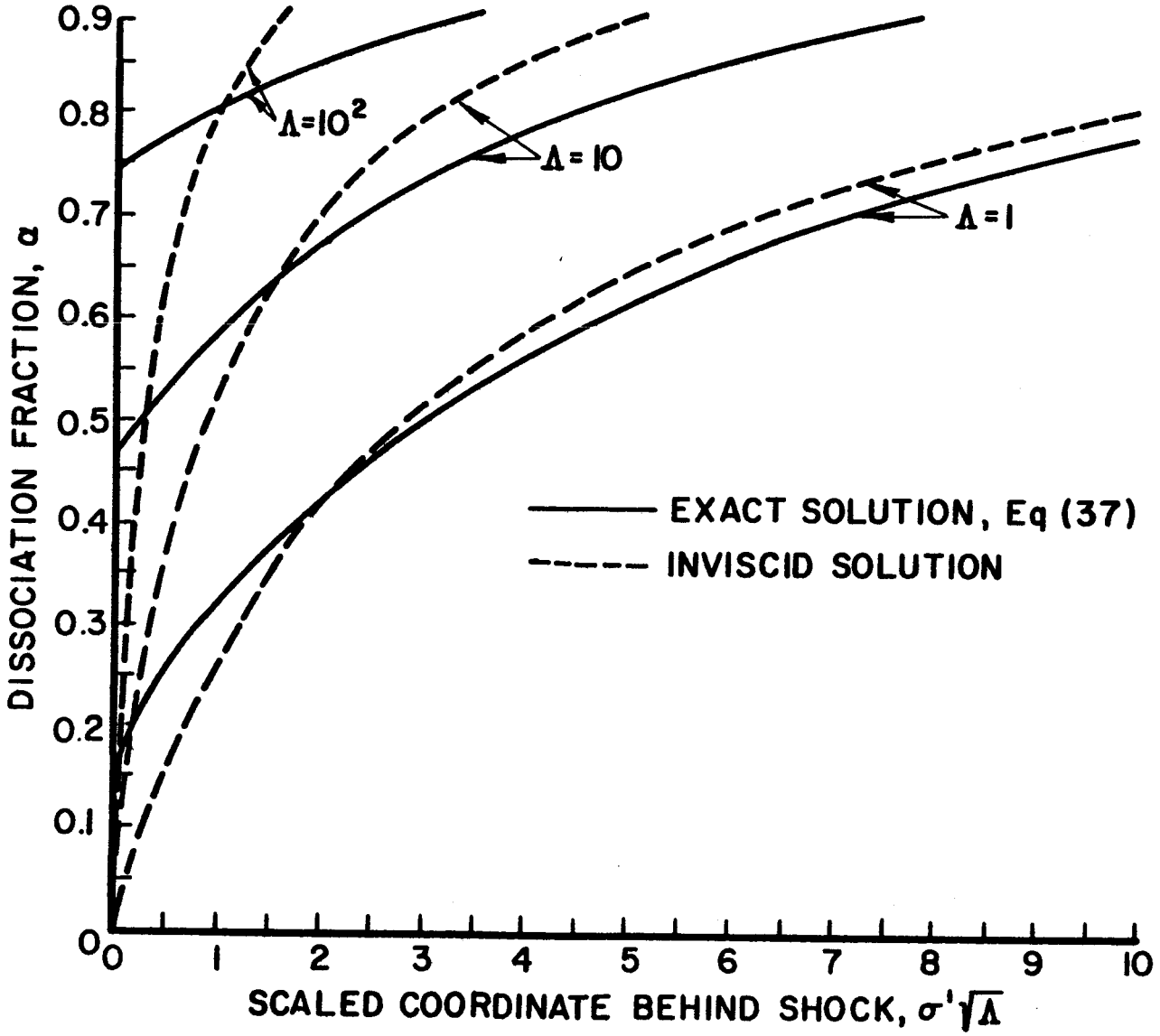

Figure 4 EFFECT OF DIFFUSION ON CONCENTRATION PROFILES FOR A LIGHTHILL GAS

$\Lambda = \bar{\Lambda} = 1$

SYMBOLS	α_{SH}	α_{∞}
———	0.17	0
△	0.27	0.13
⬭	0.37	0.27

$\bar{\Lambda} = 10$

SYMBOLS	α_{SH}	α_{∞}
– – – –	0.46	0
○	0.56	0.21
□	0.66	0.44

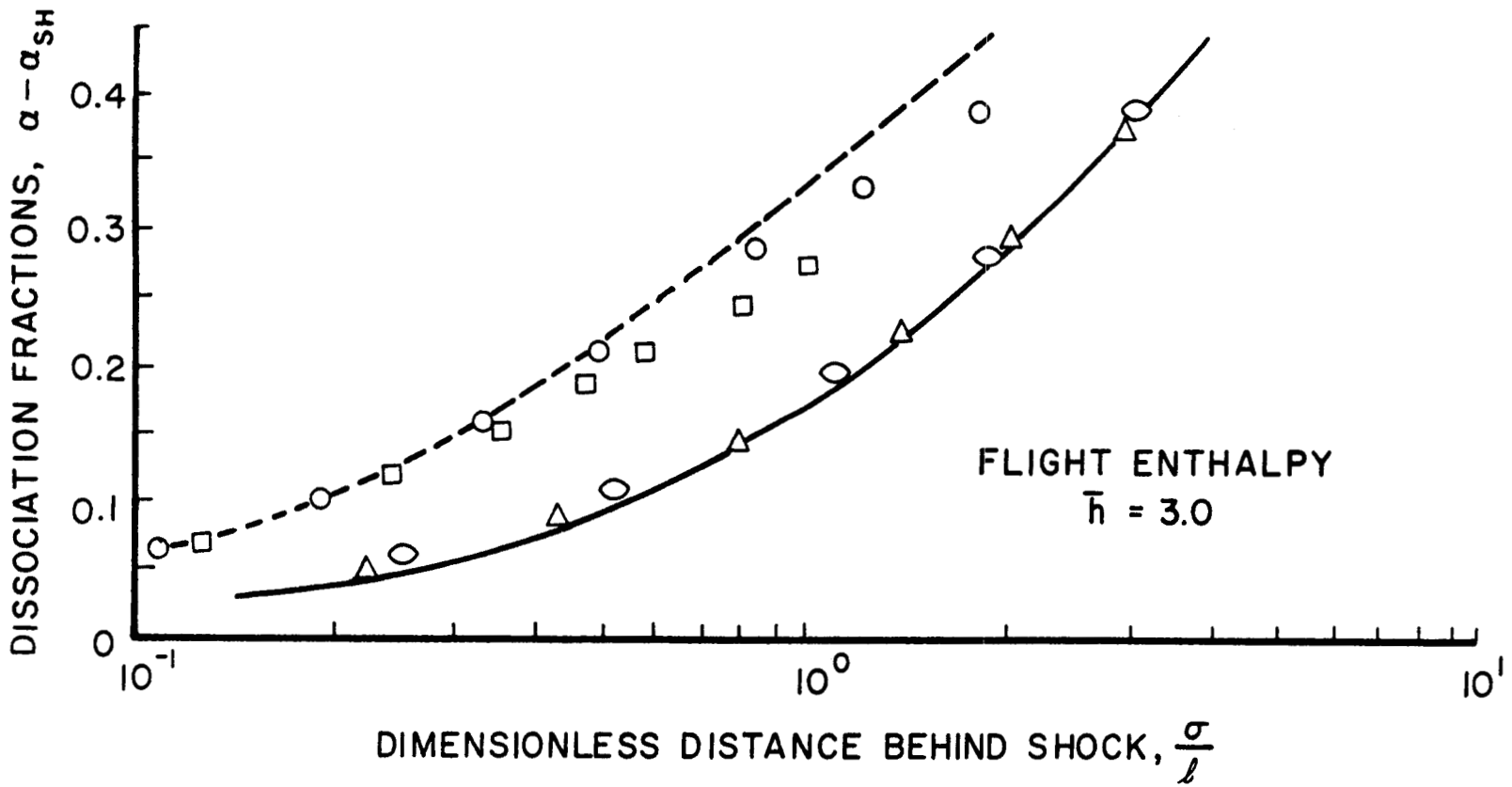

Figure 5 SUBTRACTION RULE FOR A LIGHTHILL GAS WITH DIFFUSION

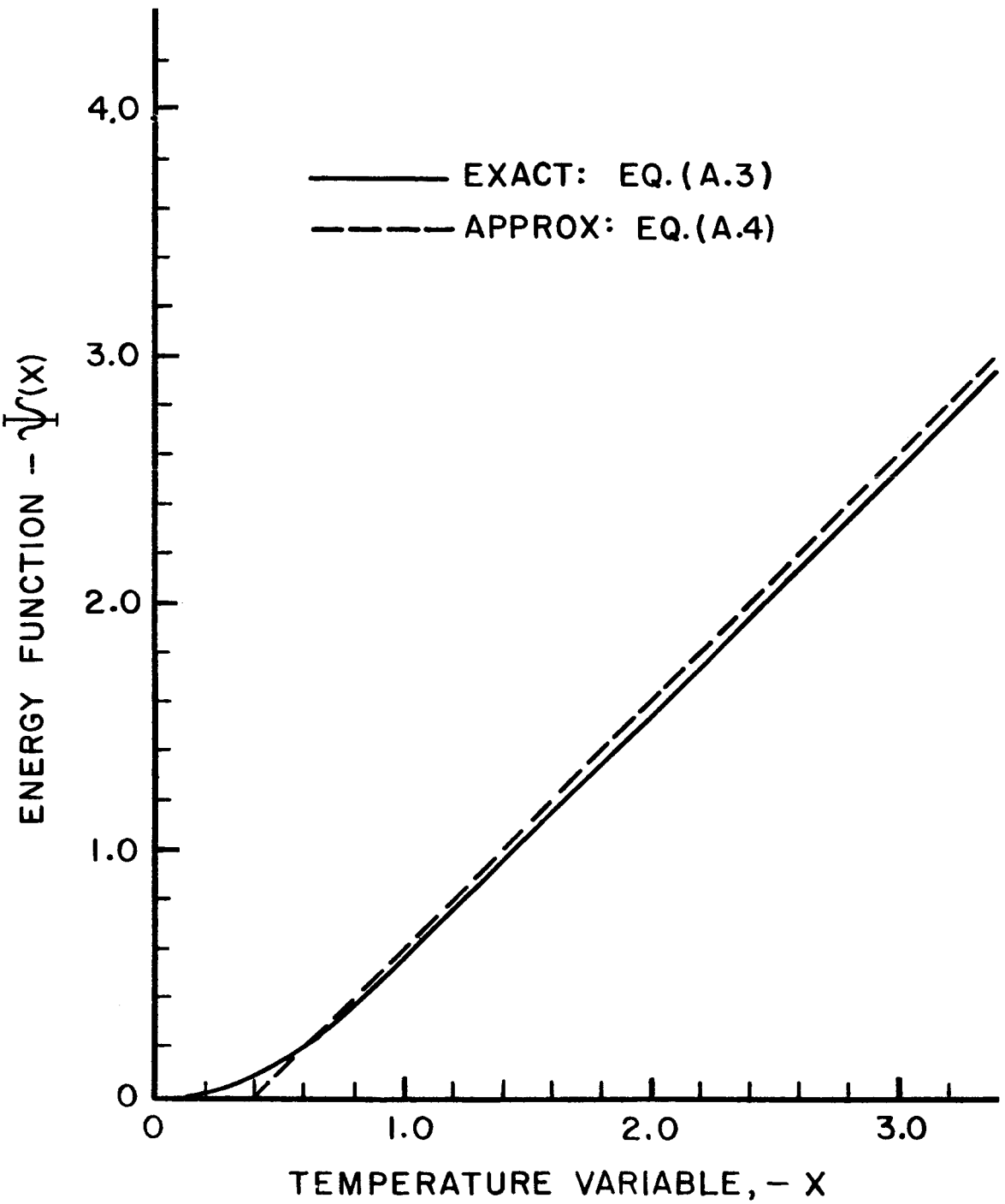

Figure A-1 LINEAR APPROXIMATION FOR THE ENERGY FUNCTION

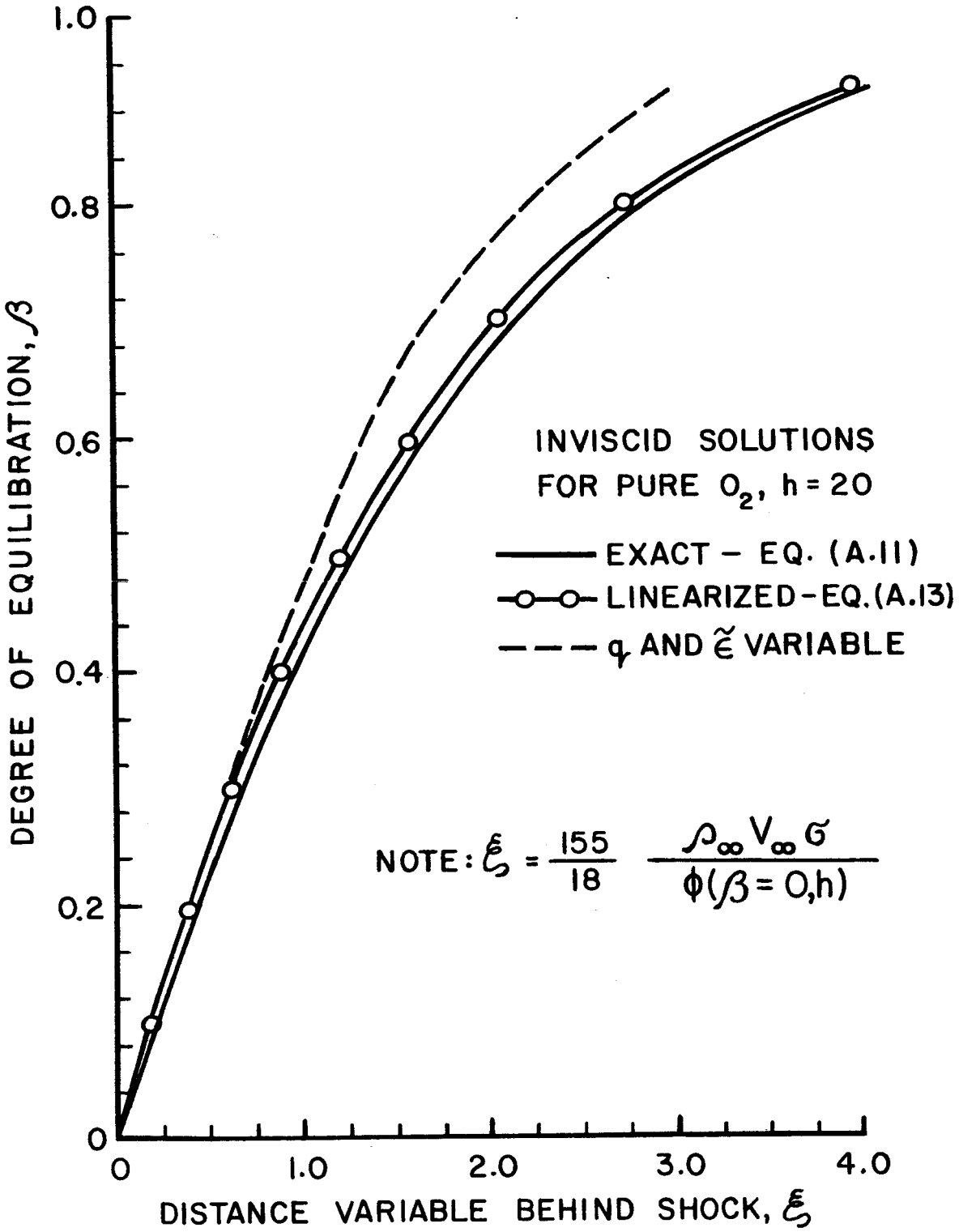

Figure A-2 COMPARISON OF LINEARIZED THEORY WITH EXACT SOLUTION

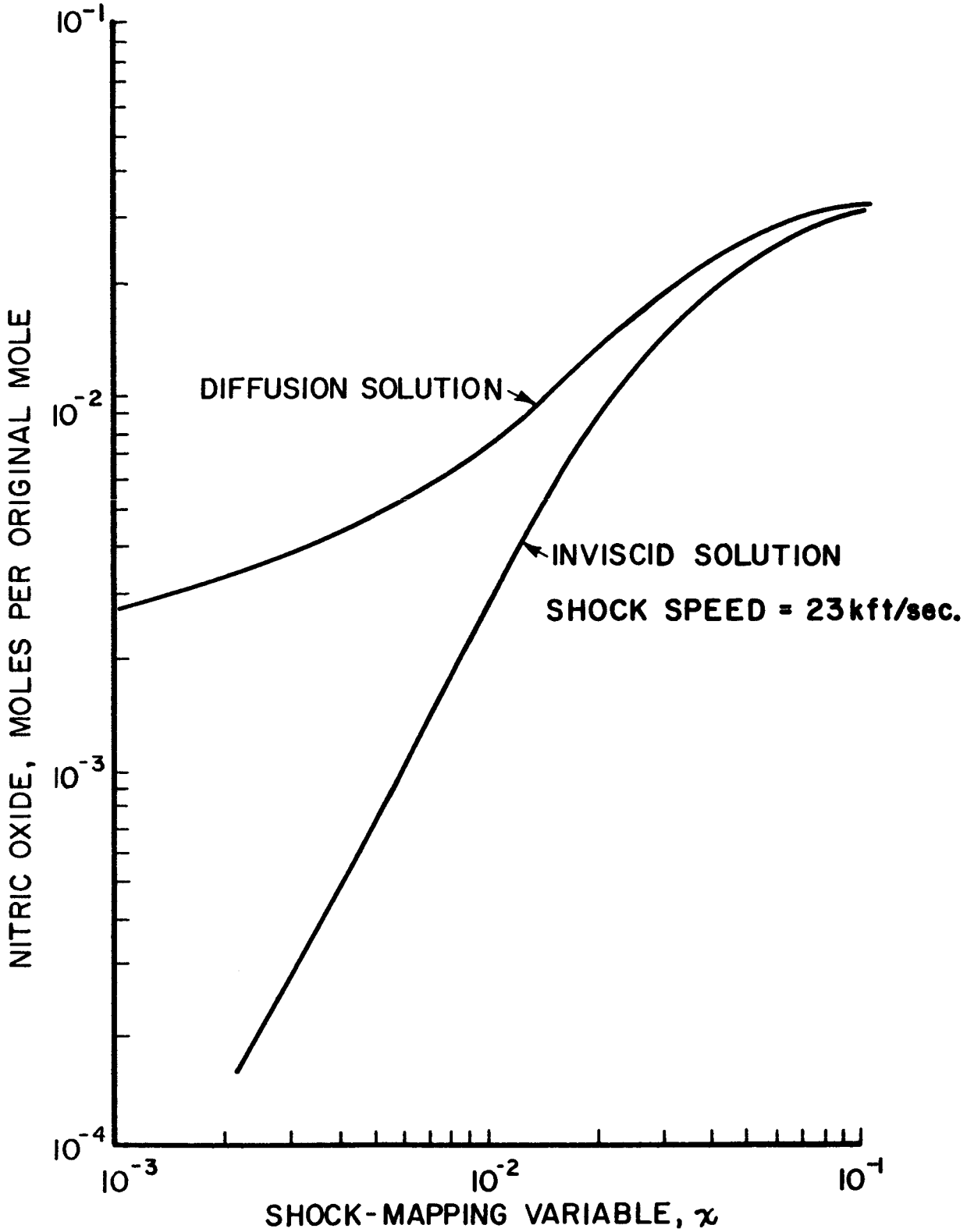

Figure B-1 EFFECT OF DIFFUSION ON NITRIC OXIDE PROFILES

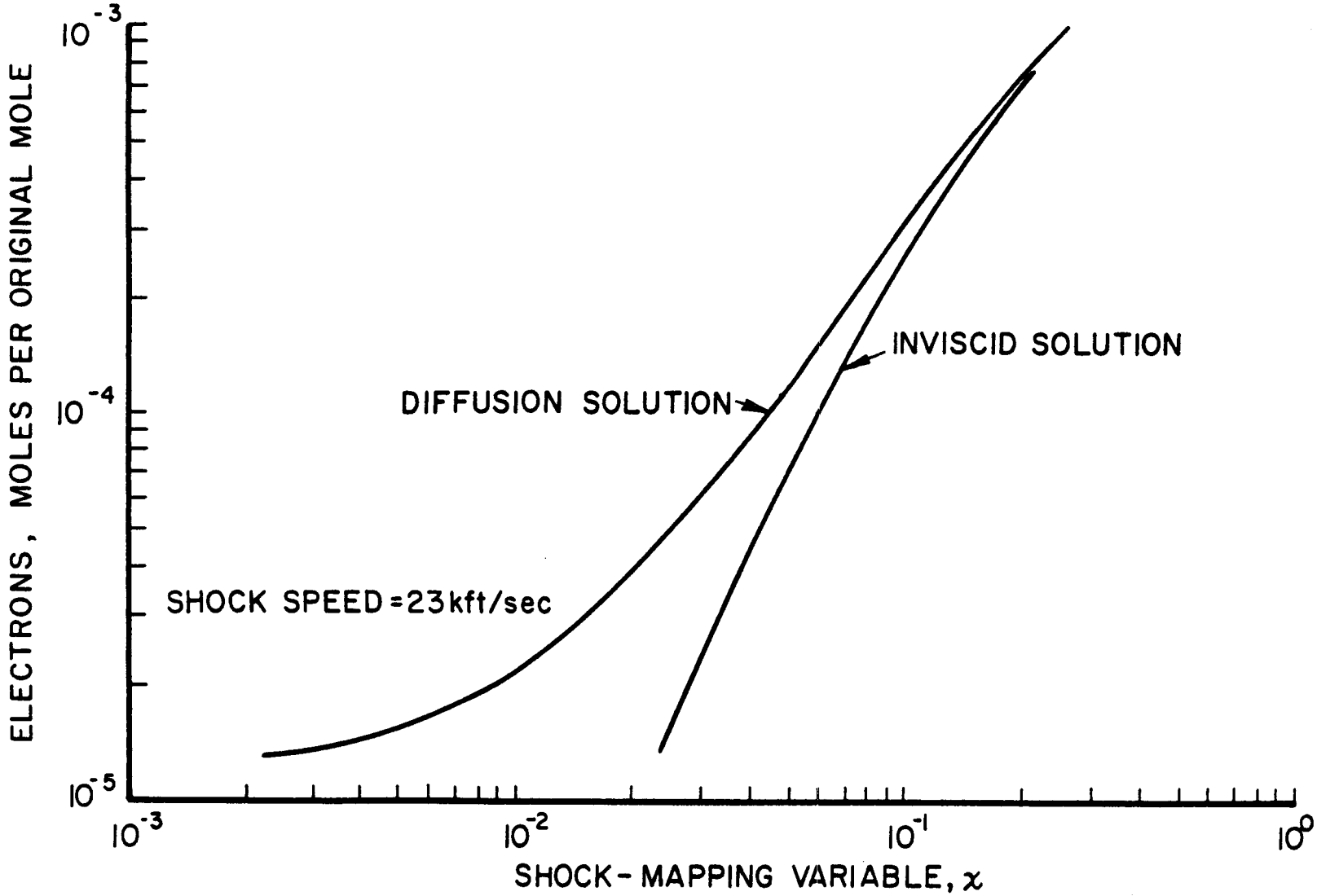

Figure B-2 EFFECT OF DIFFUSION ON ELECTRON PROFILES